Supporting Information

Unusual Dual-Emissive Heteroleptic Iridium Complexes Incorporating TADF Cyclometalating Ligands

Helen Benjamin,[a] Yonghao Zheng,[a,b] Valery N. Kozhevnikov,[a,c] Jamie S. Siddle,[a] Luke J. O'Driscoll, [a] Mark A. Fox,[a] Andrei S. Batsanov,[a] Gareth C. Griffiths,[d] Fernando B. Dias,[d] Andrew P. Monkman,[d] and Martin R. Bryce*[,a]

[a] *Department of Chemistry, Durham University, Durham DH1 3LE, U.K.* m.r.bryce@durham.ac.uk

[b] *School of Optoelectronic Science and Engineering, University of Electronic Science and Technology of China (UESTC), Chengdu 610054, China*

[c] *Department of Applied Sciences, Northumbria University, Newcastle-Upon-Tyne, NE1 8ST, U.K.*

[d] *Department of Physics, Durham University, Durham DH1 3LE, U.K.*

Contents

Synthesis of MIDA boronic esters

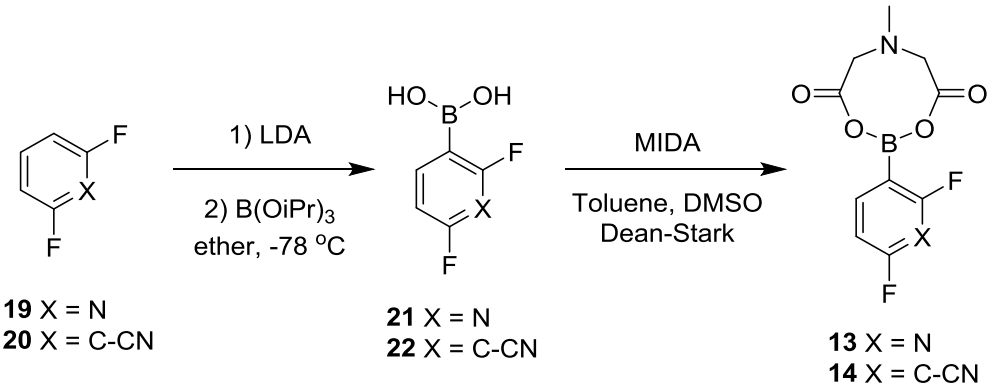

19 X = N
20 X = C-CN

21 X = N
22 X = C-CN

13 X = N
14 X = C-CN

Scheme S1: Synthesis of the required MIDA-boronic esters

2,6-Difluoro-3-pyridylboronic acid 21

^{n}BuLi (45 ml, 2.5 M in hexanes) was added dropwise to a stirred solution of DIPA (14.5 ml, 103.5 mmol) in diethyl ether (100 ml, dry) at 0 °C under argon. The solution was stirred at 0 °C for 30 min before the temperature was lowered to -78 °C. 2,6-difluoropyridine, **19** (8.5 ml, 93.7 mmol) was added dropwise and the mixture was stirred at -78 °C for 3 h. Triisopropyl borate (32.5 ml, 140.8 mmol) was slowly added, and the reaction mixture was stirred at -78 °C for 30 min before being quenched with water (100 ml) and left to warm to RT overnight. The reaction mixture was extracted with diethyl ether (3 x 50 ml) and the aqueous layer carefully acidified to pH 6 with 48% HBr. A second extraction was performed using ethyl acetate (3 x 50 ml) and the organic layers were combined and evaporated *in vacuo*. After recrystallisation from toluene, **21** was obtained as an off white powder (8.74 g, 59%); δ_H (400 MHz; d_6-acetone; Me_4Si) 8.40 (1H, q, *J* 4.5), 7.56 (2H, s), 7.04 (1H, d, *J* 8.0); δ_C (100 MHz; d_6-acetone; Me_4Si) 164.9 (dd, *J* 244.9, 14.2), 163.0 (dd, *J* 243.9, 15.2), 152.5 (t, *J* 7.9), 105.8 (dd, *J* 33.0, 5.4); δ_F (376 MHz; $CDCl_3$) -61.5 (1F, s), -68.4 (1F, s).

2,6-Difluoro-3-(6-methyl-4,8-dioxo-1,3,6,2-dioxazaborocan-2-yl)pyridine 13

A mixture of 2,6-difluoro-3-pyridylboronic acid, **21** (8.74 g, 55.0 mmol), *N*-methyliminodiacetic acid (MIDA) (8.18 g, 55.6 mmol), DMSO (45 ml), and toluene (95 ml) was heated under reflux with a Dean Stark trap overnight. After cooling to room temperature, the organic solvents were removed *in vacuo*. The product was washed with small amounts of dichloromethane, toluene and diethyl ether. **13** was obtained as a cream powder (13.33 g, 90%); δ_H (400 MHz; d_6-acetone; Me_4Si) 8.27 (1H, q, *J* 8.5), 7.08 (1H, ddd, *J*

7.6, 2.4, 1.8), 4.37 (4H, dd, *J* 97.2, 17.2), 2.98 (3H, s); δ_C (100 MHz; d_6-acetone; Me_4Si) 167.7, 164.0 (dd, *J* 240.2, 14.0), 162.9 (dd, *J* 243.1, 15.5), 151.5 (t, *J* 8.0), 106.0 (dd, *J* 32.9, 5.2), 62.7, 47.3; δ_B (128 MHz; d_6-acetone) 10.7 (br s).

2,4-Difluoro-3-cyanophenylboronic acid 22

^{n}BuLi (13.8 ml, 2.5 M in hexanes) was added dropwise to a stirred solution of DIPA (5.24 ml, 37.3 mmol) in THF (40 ml, dry) at 0 °C under argon. The solution was stirred at 0 °C for 30 min before the temperature was lowered to -78 °C. A solution of 2,6-difluorobenzonitrile **20** (4.00 g, 28.8 mmol) in THF (15 ml, dry) was added dropwise via cannula and the mixture was stirred at -78 °C for 1 h. Triisopropyl borate (9.95 ml, 43.1 mmol) was slowly added, and the reaction mixture was stirred at -78 °C for 1 h before being left to warm to RT overnight. Dilute HCl was added and the solution was extracted with EtOAc. The solvent was removed *in vacuo* to leave a sticky brown solid. The solid was redissolved in EtOAc and extracted with aqueous KOH (150 ml). The aqueous layer was acidified to pH 5 with dilute HCl and extracted with EtOAc. The solvent was removed *in vacuo* to give a beige solid, 2,4-difluoro-3-cyanophenylboronic acid **22** (4.39 g, 84%); δ_H (400 MHz; acetone-d_6; Me_4Si) 8.13 (1H, dt, *J* 8.6 7.1), 7.71 (2H, s), 7.32 (1H, td, *J* 8.6 0.9); δ_F (376 MHz; acetone-d_6; Me_4Si) -98.62 (1F, d, *J* 6.6), -105.73 (1F, t, *J* 7.6); δ_B (400 MHz; acetone-d_6; Me_4Si) 27.22 (1B, s); NMR data are consistent with the literature data.[S1]

2,6-Difluoro-3-(6-methyl-4,8-dioxo-1,3,6,2-dioxazaborocan-2-yl)benzonitrile 14

A mixture of **22** (4.39 g, 24.0 mmol), *N*-methyliminodiacetic acid (MIDA) (4.24 g, 28.8 mmol), DMSO (40 ml), and toluene (80 ml) was heated under reflux with a Dean Stark trap overnight. The mixture was cooled to room temperature, and water (50 ml) was added. The precipitate was filtered off, washed with water and dried under vacuum to give **14** as an off-white solid (5.10 g, 72%); δ_H (400 MHz; $CDCl_3$; Me_4Si) 7.82 (1H, q, *J* 7.5), 7.39 (1H, t, *J* 8.7), 4.40 (2H, d, *J* 17.3), 4.08 (2H, d, *J* 17.3), 2.62 (3H, s); δ_F (376 MHz; DMSO-d_6; Me_4Si) -97.74 (d, *J* 7.6), -104.91 (ddt, *J* 11.1, 6.6, 3.1); NMR data are consistent with the literature data.[S1]

Mass spectrometry of complexation reactions

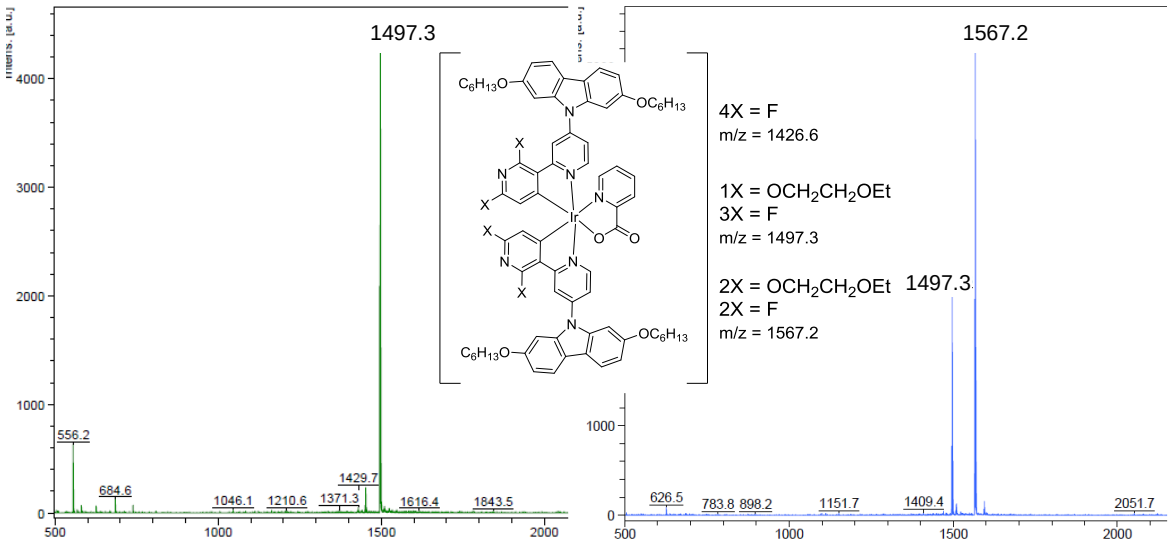

Figure S1: Mass spectra (MALDI-TOF) of two products isolated from the reaction of **10** with $IrCl_3.3H_2O$ and picolinic acid in ethoxyethanol at 130 ^oC.

X-ray crystallography

Table S1: Crystal data

Compound	**2**	**3**
CCDC	1962578	1962579
Formula	$C_{44}H_{34}F_4IrN_5O_2 \cdot 1.5\ C_6H_{14}$	$C_{48}H_{34}F_4IrN_5O_2 \cdot 4\ CDCl_3$
$D_{calc.}$/ g cm^{-3}	1.480	1.693
μ/mm^{-1}	2.86	2.94
Formula Weight	1062.22	1462.50
Size/mm^3	0.08×0.13×0.23	0.06×0.08×0.10
T/K	120	120
Crystal System	triclinic	triclinic
Space Group	$P\bar{1}$ (no. 2)	$P\bar{1}$ (no. 2)
a/Å	12.7261(3)	10.0759(5)
b/Å	14.9853(4)	16.3073(8)
c/Å	15.3107(4)	17.9412(8)
α/°	60.976(1)	89.3872(15)
β/°	80.336(1)	76.7980(14)
γ/°	69.010(1)	89.1792(15)
V/Å^3	2383.7(1)	2869.64
Z	2	2
Wavelength/Å	0.71073	0.71073
Θ_{max}/°	60	58.3
Reflections measured	43050	59027
unique	13914	15449
with I>2σ(I)	12256	12529
R_{int}	0.035	0.059
Parameters/restraints	517/0	701/52
wR_2 (all data)	0.065	0.077
R_1 [I>2σ(I)]	0.026	0.036

X-ray diffraction experiments were carried out on Bruker 3-circle diffractometers SMART 6000 with a CCD area detector, using graphite-monochromated sealed-tube Mo-$K\alpha$ radiation (**2**) and D8 Venture with a PHOTON 100 CMOS area detector, using Mo-$K\alpha$ radiation from an Incoatec IμS microsource with focusing mirrors (**3**). The crystals were cooled using a Cryostream 700 (Oxford Cryosystems) open-flow N2 gas cryostat. The data were corrected for absorption by numerical integration based on the crystal face-indexing. Structure **2** was solved by direct methods using SHELXS 2013/1 program[S2], structure **3** by dual-space intrinsic phasing method using SHELXT 2018/2 program[S3], both were refined by full-matrix least squares using SHELXS 2018/3 program[S4] on Olex2 platform[S5]. Structure **2** contains infinite channels parallel to the [1 1 0] direction, comprising 28% of the crystal space (705 Å^3 per unit cell) and occupied by disordered solvent (observe integral electron density 151 e per unit cell, presumably ca. 3 molecules of hexane) which was masked using SMTBX program in OLEX2[S6].

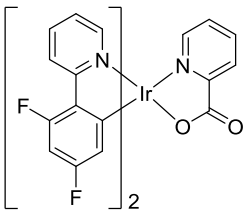

FIrpic

Figure S2: Structure of **FIrpic**.

Table S2: Selected bond distances (Å)

	FIrpic[a,b]	**1**[b,c]	**2**	**3**
Ir-N(1)	2.048[11]	2.040(2)	2.040(2)	2.046(2)
Ir-N(2)	2.041[8]	2.037(2)	2.032(2)	2.033(2)
Ir-N(3)	2.140[8]	2.143(2)	2.123(2)	2.123(3)
Ir-O(1)	2.154[7]	2.163(2)	2.110(2)	2.147(2)
Ir-C(1)	2.000[8]	2.001(2)	1.989(3)	1.996(3)
Ir-C(21)	1.991[9]	1.988(3)	1.982(2)	1.987(3)

[a] Weighted average from six X-ray structure determinations[S7–S11]; [b] Atom numbering in Table S2 is consistent with Figure 1 in the manuscript; [c] ref.[S12]

Cyclic voltammetry

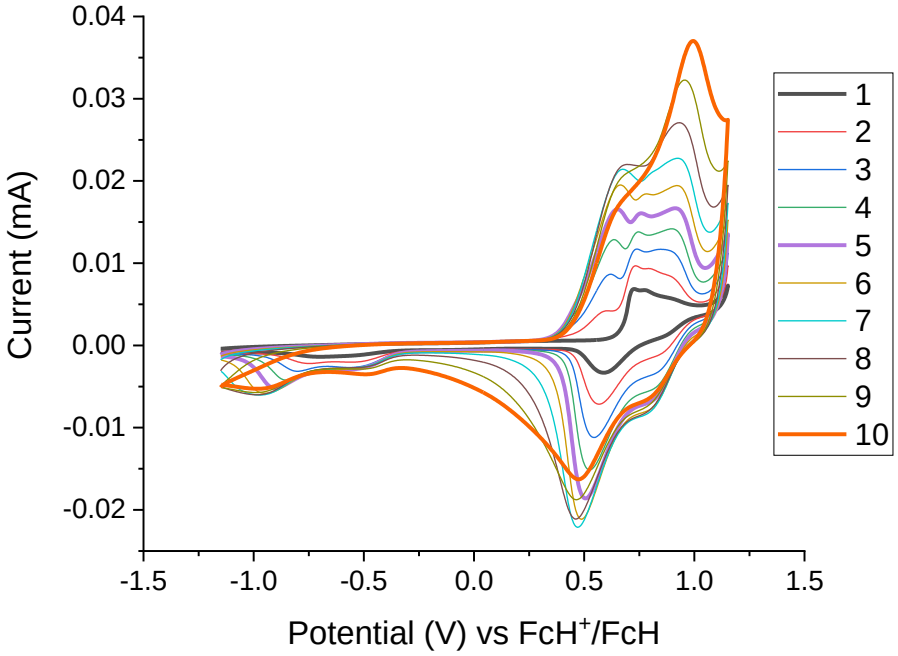

Figure S3: Cyclic voltammogram of 10 successive scans of complex **4** at 100 mV/s.

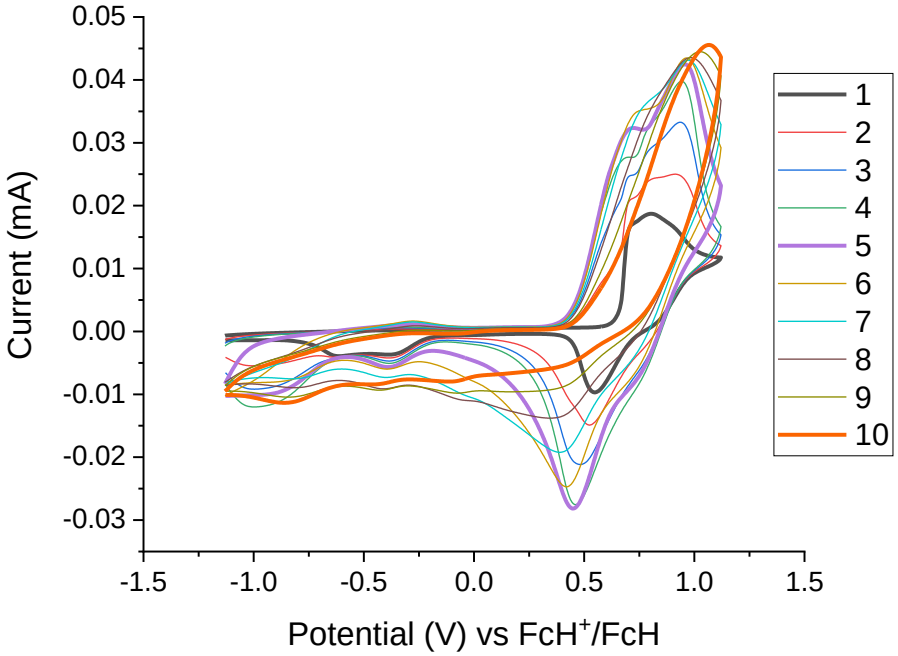

Figure S4: Cyclic voltammogram of 10 successive scans of complex **5** at 100 mV/s.

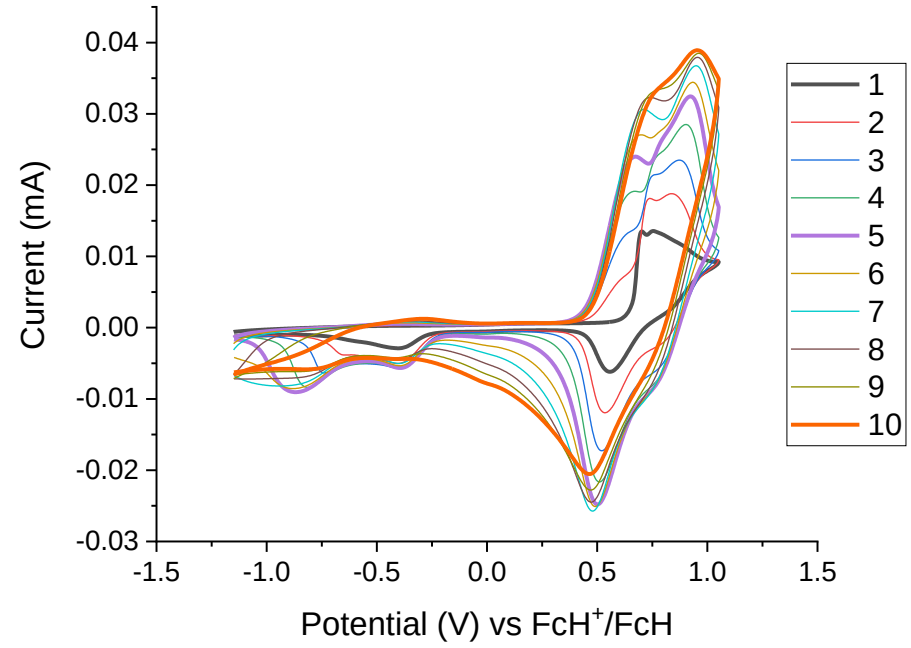

Figure S5: Cyclic voltammogram of 10 successive scans of complex **6** at 100 mV/s.

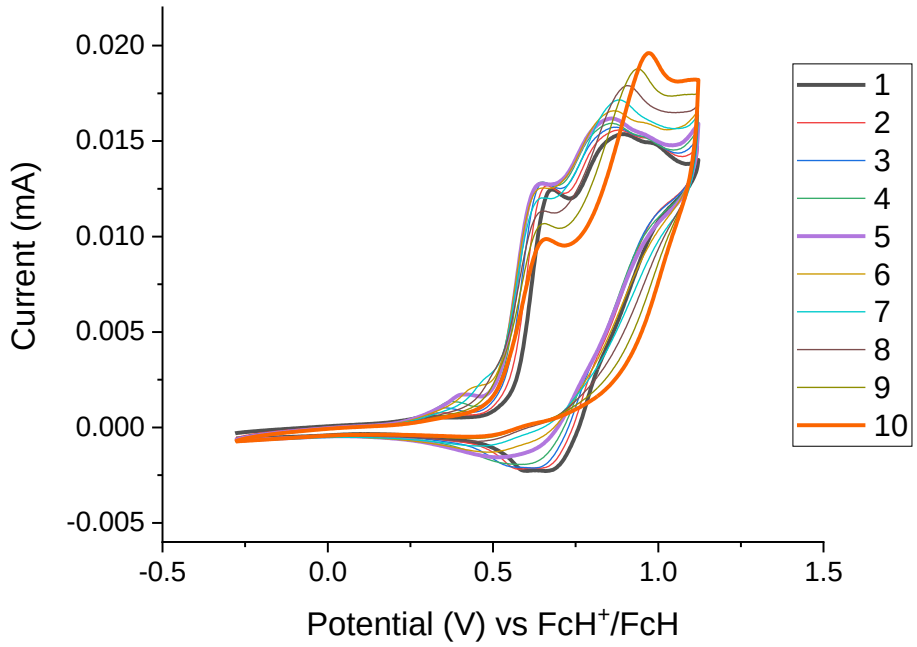

Figure S6: Cyclic voltammogram of 10 successive scans of ligand **9** at 100 mV/s.

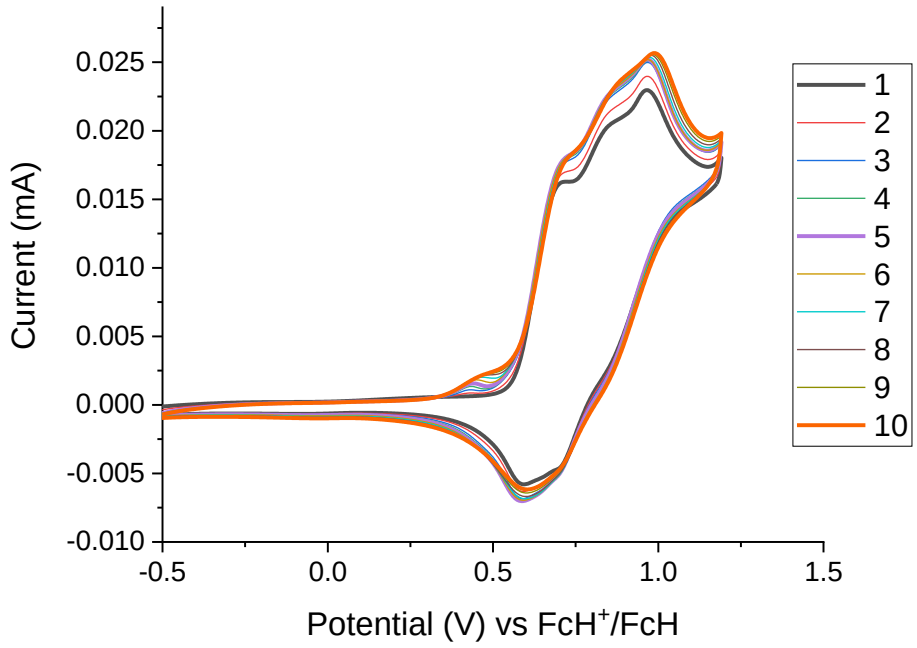

Figure S7: Cyclic voltammogram of 10 successive scans of ligand **10** at 100 mV/s.

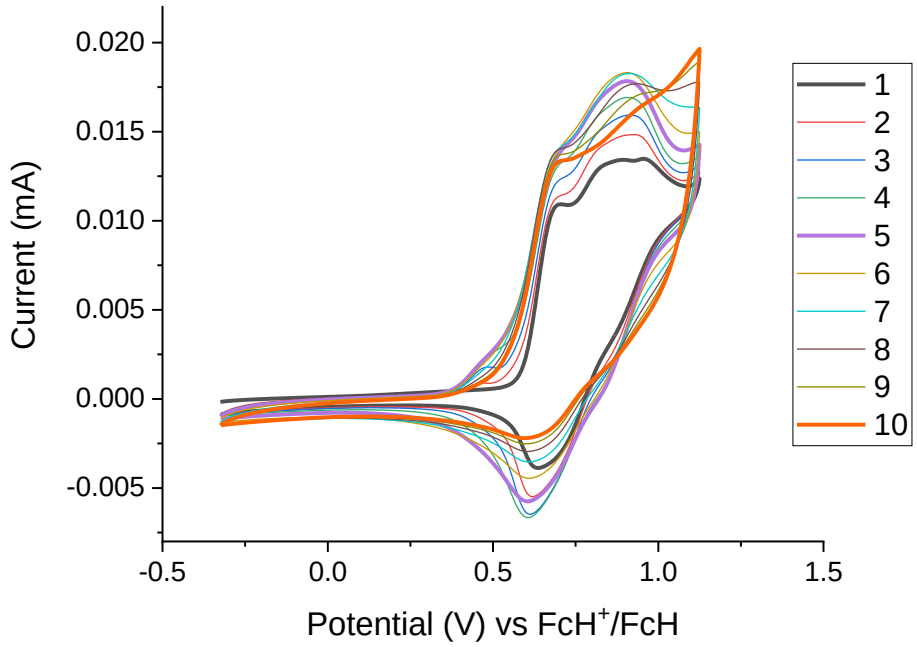

Figure S8: Cyclic voltammogram of 10 successive scans of ligand **11** at 100 mV/s.

Photophysics

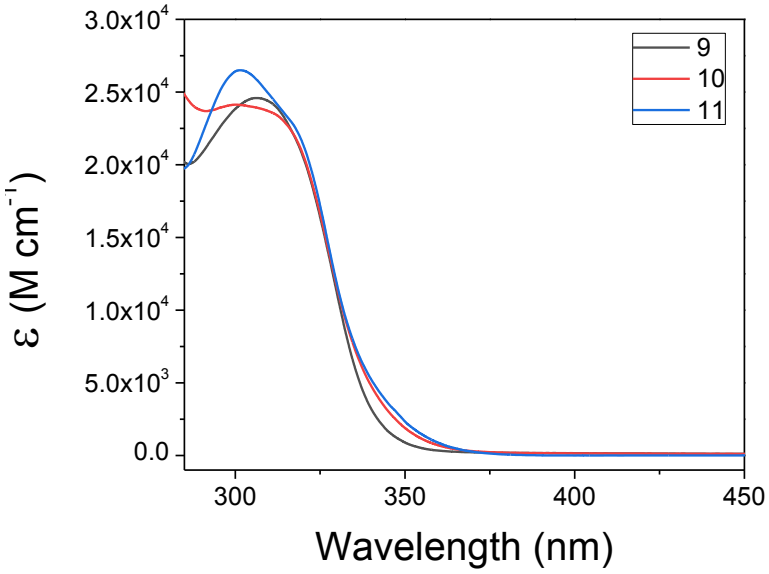

Figure S9: Absorption spectra of ligands **9-11** in toluene (< 5 x 10^{-5} M).

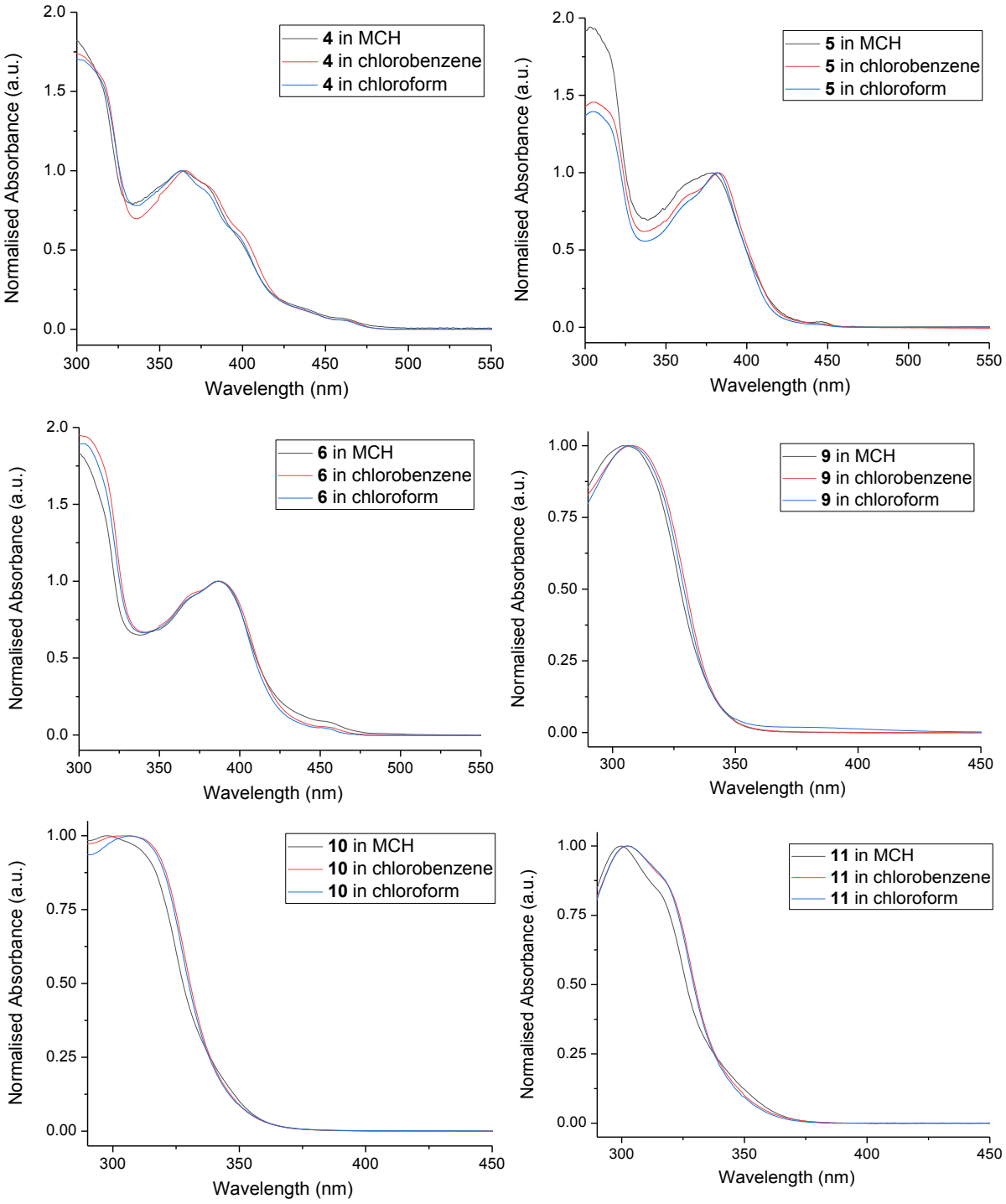

Figure S10: Absorption spectra of dual emissive complexes **4**-**6**, and ligands **9**-**11** in different solvents [< 10^{-5} M]. MCH = methylcyclohexane.

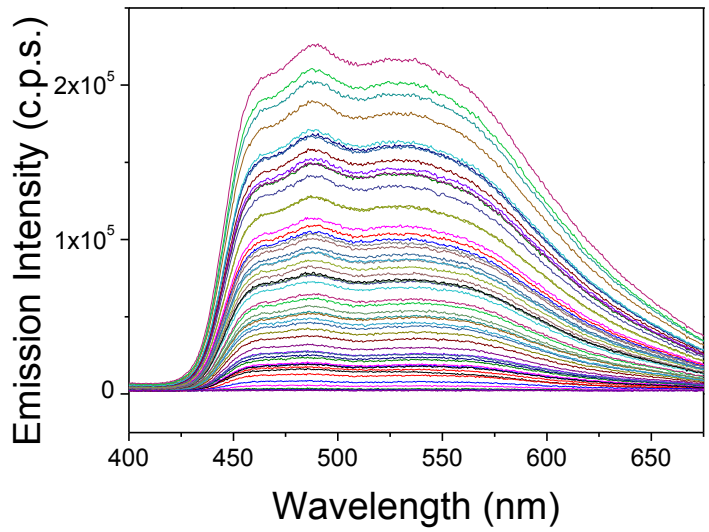

Figure S11: The decay profile of complex **5** in chlorobenzene (λ_{ex} = 355 nm) (< 5 x 10^{-5} M).

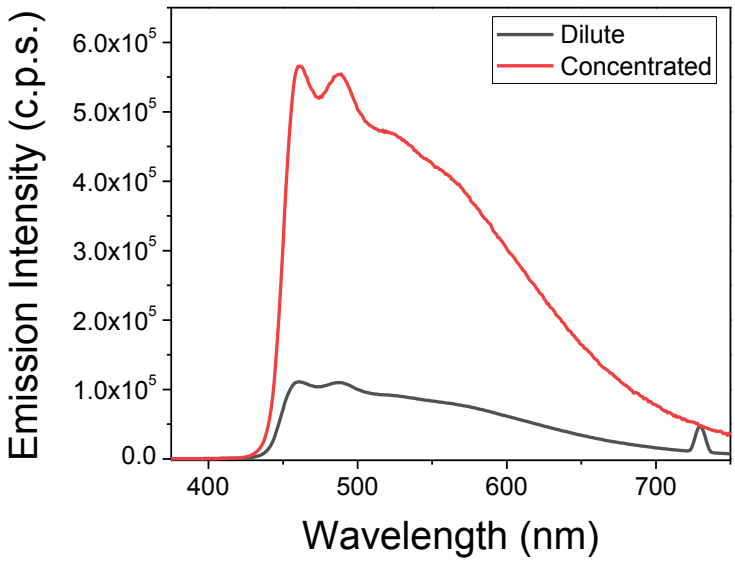

Figure S12: Emission spectra of concentrated (10^{-4} M) and dilute (10^{-5} M) solutions of **5** in chlorobenzene (λ_{ex} = 365 nm).

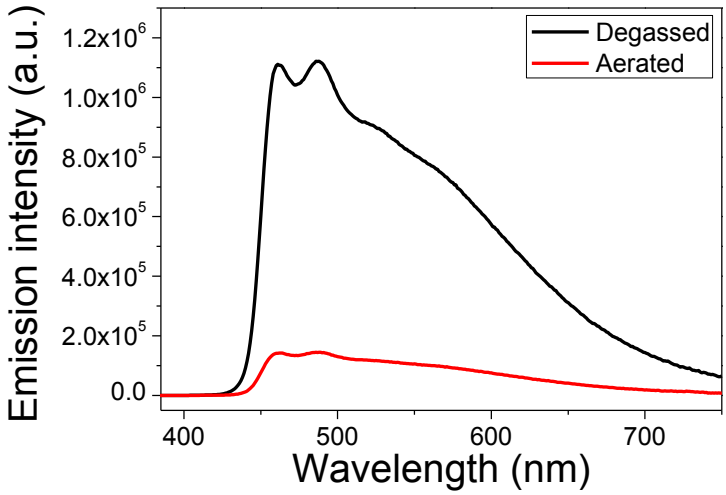

Figure S13: Emission of **5** in degassed and aerated chlorobenzene (λ_{ex} = 365 nm).

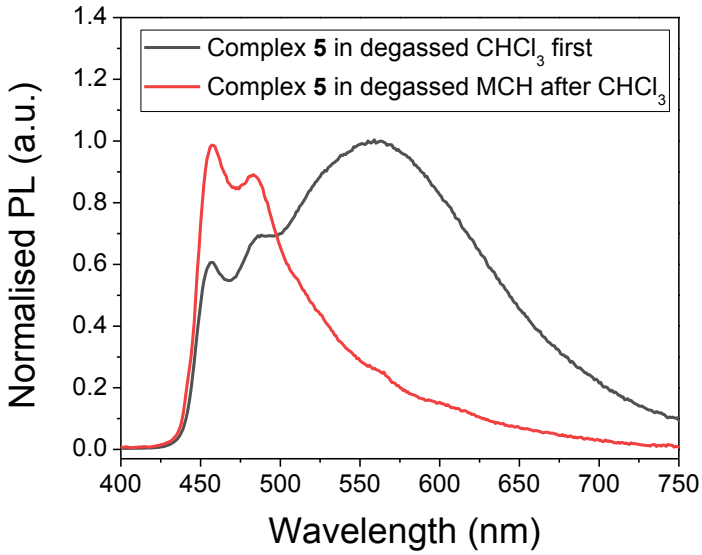

Figure S14: Degradation test: Emission of **5** in degassed $CHCl_3$. The solvent was the removed and the residue was then re-dissolved in MCH (degassed). λ_{ex} = 365 nm.

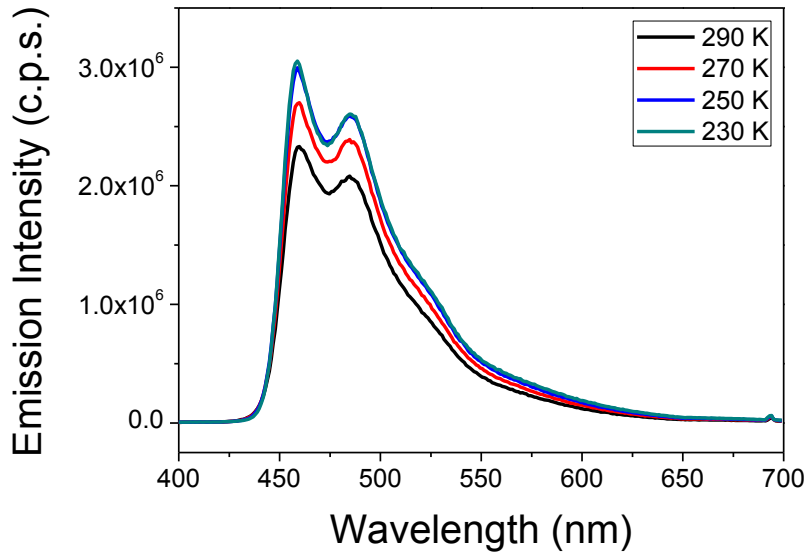

Figure S15: Emission of **5** in zeonex films.

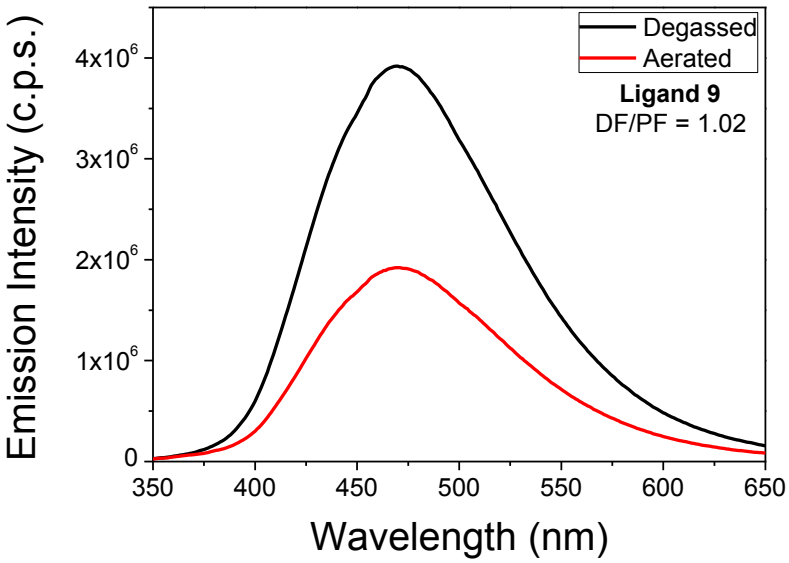

Figure S16: Emission of ligand **9** in degassed and aerated chlorobenzene (λ_{ex} = 340 nm). DF/PF = the ratio between delayed and prompt emission, calculated from the following:

$$\frac{\int I_{DF}^{deg}(\lambda)d\lambda}{\int I_{PF}^{O2}(\lambda)d\lambda} = \frac{\Phi_{PF}+\Phi_{DF}}{\Phi_{PF}} = 1 + \frac{\Phi_{DF}}{\Phi_{PF}}.$$

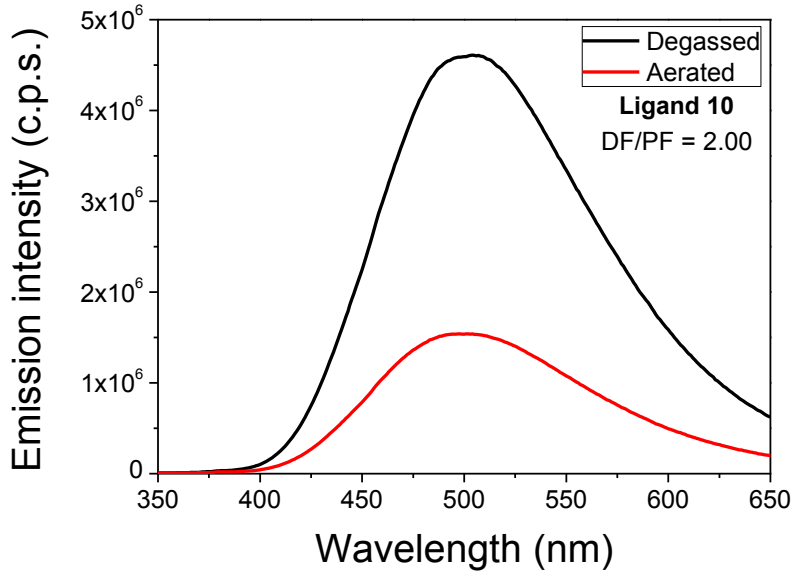

Figure S17: Emission of ligand **10** in degassed and aerated chlorobenzene (λ_{ex} = 340 nm). DF/PF = the ratio between delayed and prompt emission, calculated from the following:

$$\frac{\int I_{DF}^{deg}(\lambda)d\lambda}{\int I_{PF}^{O2}(\lambda)d\lambda} = \frac{\Phi_{PF}+\Phi_{DF}}{\Phi_{PF}} = 1 + \frac{\Phi_{DF}}{\Phi_{PF}}.$$

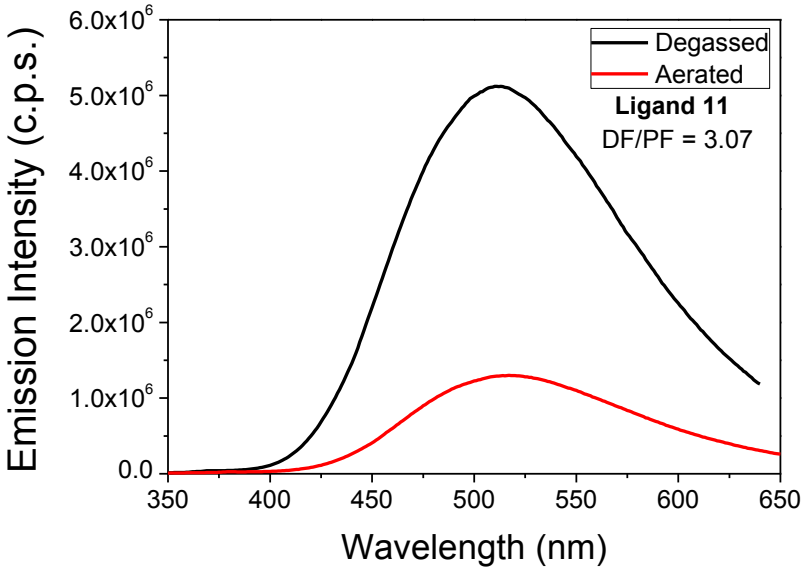

Figure S18: Emission of ligand **11** in degassed and aerated chlorobenzene (λ_{ex} = 340 nm). DF/PF = the ratio between delayed and prompt emission, calculated from the following:

$$\frac{\int I_{DF}^{deg}(\lambda)d\lambda}{\int I_{PF}^{O2}(\lambda)d\lambda} = \frac{\Phi_{PF}+\Phi_{DF}}{\Phi_{PF}} = 1 + \frac{\Phi_{DF}}{\Phi_{PF}}.$$

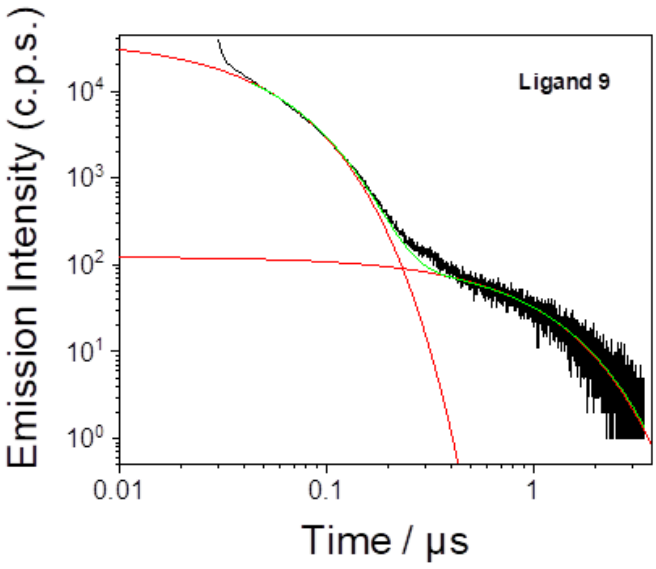

Equation	y = A1*exp(-x/t1) + A2*exp(-x/t2) + y0
Plot	E
y0	0 ± 0
A1	37662.37912 ± 24.48561
t1	0.039 ± 0
A2	119.52 ± 0
t2	0.76762 ± 0
Reduced Chi-Sqr	1536.586
R-Square (COD)	0.9983
Adj. R-Square	0.9983

Figure S19: Emission lifetime of ligand **9** in degassed chlorobenzene (λ_{ex} = 340 nm). Fittings of individual decay components shown in red, fitting of the total decay shown in green.

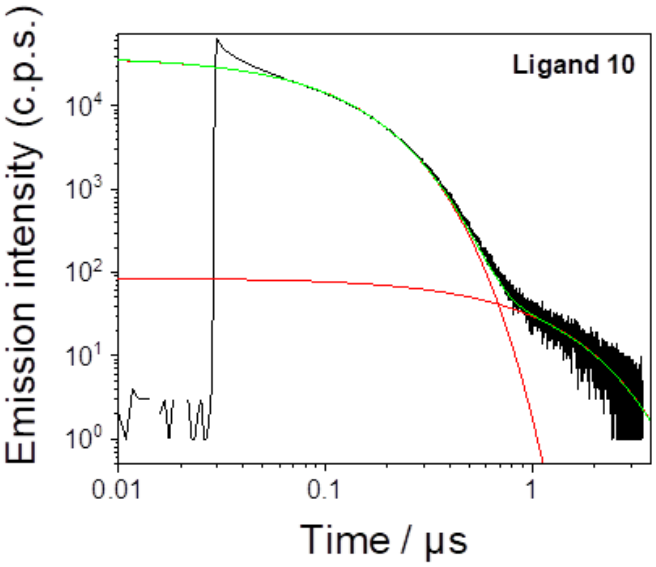

Equation	y = A1*exp(-x/t1) + A2*exp(-x/t2) + y0
Plot	Decay
y0	0 ± 0
A1	39245.73951 ± 36.27786
t1	0.09947 ± 7.6519E-5
A2	85 ± 0
t2	0.946 ± 0
Reduced Chi-Sqr	4143.207
R-Square (COD)	0.99937
Adj. R-Square	0.99937

Figure S20: Emission lifetime of ligand **10** in degassed chlorobenzene (λ_{ex} = 340 nm). Fittings of individual decay components shown in red, fitting of the total decay shown in green.

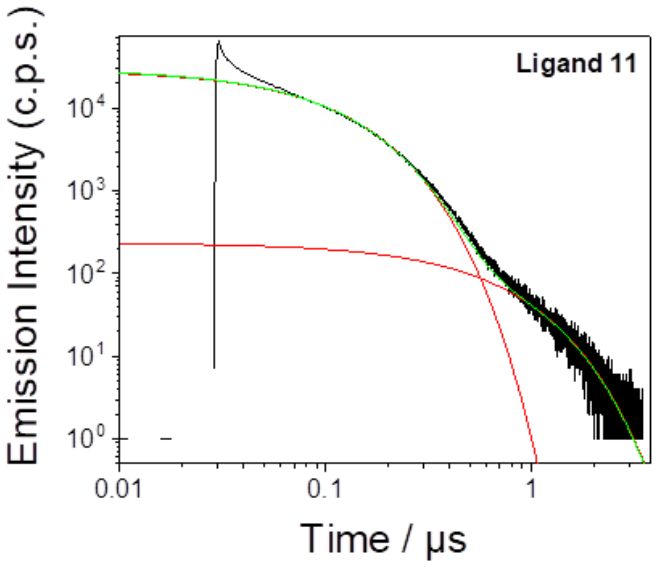

Equation	y = A1*exp(-x/t1) + A2*exp(-x/t2) + y0
Plot	Decay
y0	0 ± 0
A1	29434.19468 ± 35.66585
t1	0.09408 ± 8.78317E-5
A2	233 ± 0
t2	0.57 ± 0
Reduced Chi-Sqr	2631.265
R-Square (COD)	0.99915
Adj. R-Square	0.99915

Figure S21: Emission lifetime of ligand **11** in degassed chlorobenzene (λ_{ex} = 340 nm). Fittings of individual decay components shown in red, fitting of the total decay shown in green.

DFT calculations

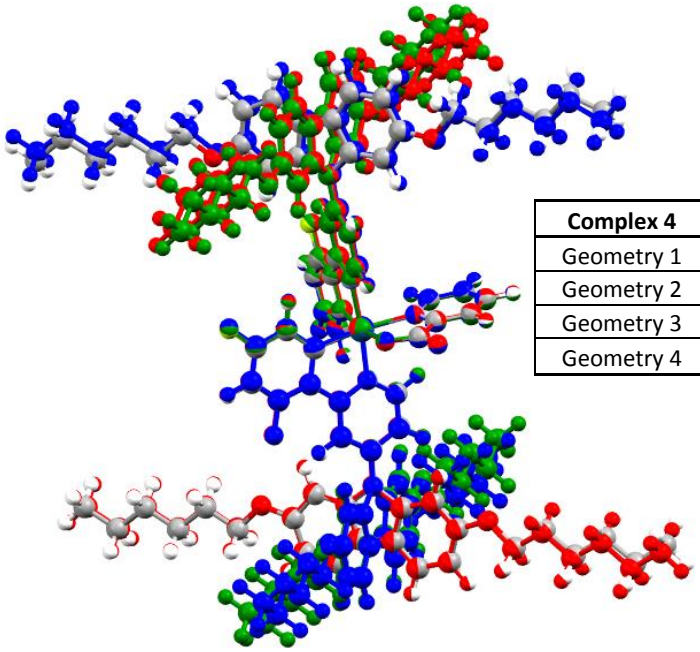

	Energy of S_0	
Complex 4	kJ/mol	Difference in kJ/mol
Geometry 1	-10841593.55	0.00
Geometry 2	-10841593.64	-0.09
Geometry 3	-10841593.31	0.33
Geometry 4	-10841593.36	0.19

Figure S22: Geometries of the three ground states found for complex **4**. Geometry 1 is coloured by element, Geometry 2 is coloured red, Geometry 3 is coloured in blue, Geometry 4 is coloured in green.

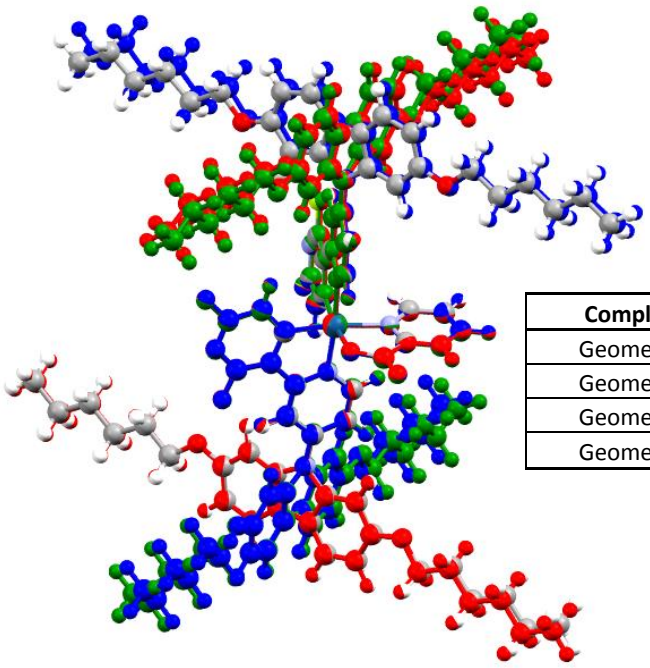

	Energy of S_0	
Complex 5	kJ/mol	Difference in kJ/mol
Geometry 1	-10924950.79	0.00
Geometry 2	-10924950.85	-0.07
Geometry 3	-10924950.92	-0.13
Geometry 4	-10924950.65	0.20

Figure S23: Geometries of the three ground states found for complex **5**. Geometry 1 is coloured by element, Geometry 2 is coloured red, Geometry 3 is coloured in blue, Geometry 4 is coloured in green.

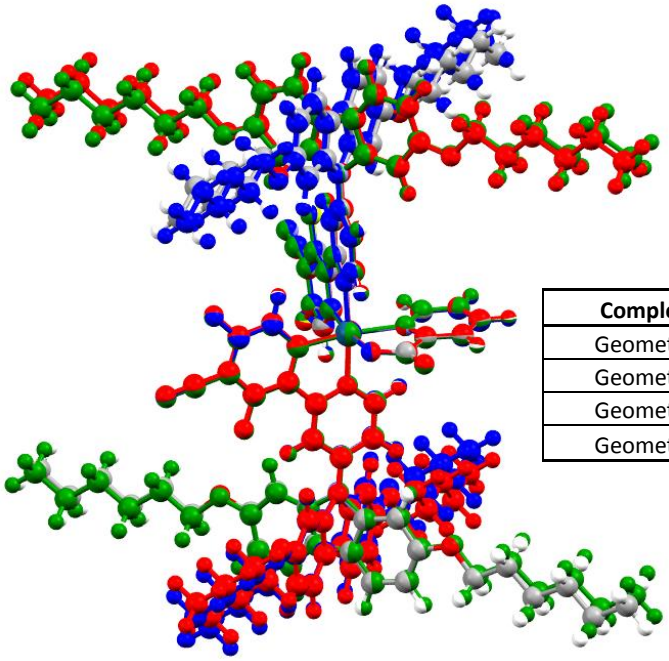

	Energy of S_0	
Complex 6	kJ/mol	Difference in kJ/mol
Geometry 1	-11320866.67	0.00
Geometry 2	-11320866.83	-0.16
Geometry 3	-11320866.72	-0.05
Geometry 4	-11320866.50	0.33

Figure S24: Geometries of the three ground states found for complex **6**. Geometry 1 is coloured by element, Geometry 2 is coloured red, Geometry 3 is coloured in blue, Geometry 4 is coloured in green.

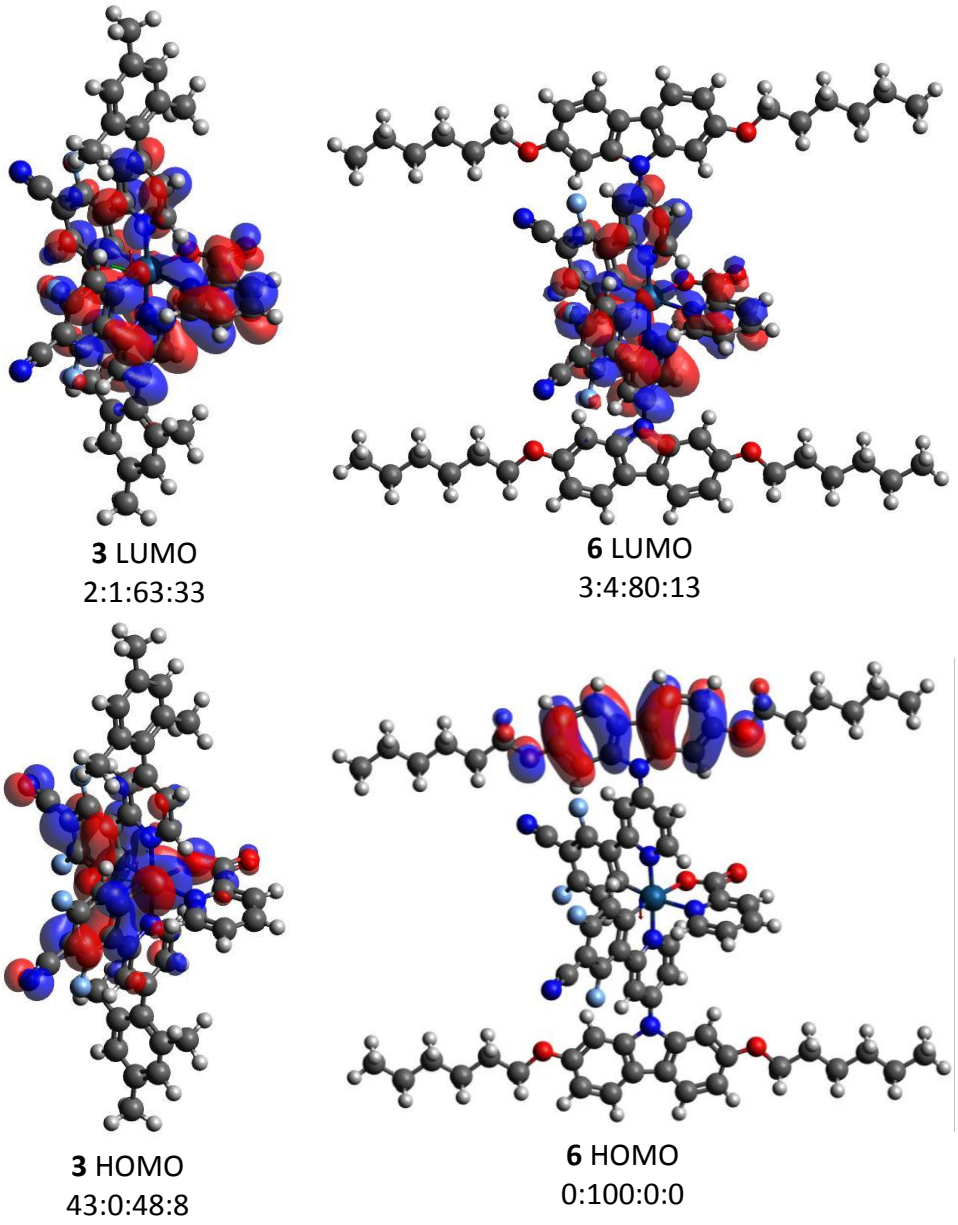

Figure S25: Frontier molecular orbitals for **3** and **6**. Isocontours set to ±0.02 e/bohr^3. Ir:mesityl/carbazolyl:phenylpyridyl:picolyl % orbital contribution ratio listed for each orbital.

Table S3: *Energy and Distribution of Complex **2** Frontier Orbitals*

MO	eV	Ir	mesityl1	pyridine1	phenyl1	mesityl2	pyridine2	phenyl2	pic
L+5	-1.16	2	1	45	7	0	10	2	33
L+4	-1.19	2	1	27	3	1	55	7	4
L+3	-1.42	1	0	12	2	0	19	3	62
L+2	-1.85	4	1	53	21	0	12	5	2
L+1	-1.91	5	0	5	3	1	36	18	32
LUMO	-1.99	1	0	8	4	0	15	7	64
HOMO	-6.13	52	0	5	14	0	4	14	12
H-1	-6.19	50	0	7	4	0	2	6	30
H-2	-6.61	45	6	2	4	14	13	11	5
H-3	-6.61	3	91	3	0	2	1	1	0
H-4	-6.63	9	0	0	1	82	4	2	1
H-5	-6.67	1	94	2	3	0	0	0	1

Table S4*: Energy and Distribution of Complex **3** Frontier orbitals*

MO	eV	Ir	mesityl1	pyridine1	phenyl1	mesityl2	pyridine2	phenyl2	pic
L+5	-1.27	2	1	28	6	1	47	8	8
L+4	-1.29	2	0	5	14	0	7	57	15
L+3	-1.5	1	0	14	5	1	21	10	48
L+2	-1.94	5	1	50	22	0	12	5	5
L+1	-1.99	5	0	1	0	1	22	12	60
LUMO	-2.07	2	0	13	7	1	28	15	33
HOMO	-6.04	43	0	3	21	0	3	21	8
H-1	-6.26	52	0	8	2	0	2	3	33
H-2	-6.65	0	97	3	0	0	0	0	0
H-3	-6.66	1	0	0	0	96	3	0	0
H-4	-6.7	31	36	2	5	5	9	7	4
H-5	-6.7	21	62	0	1	4	5	4	2

Table S5: *Complex **4**, Geometry 1 - Frontier orbital energies and distributions*

MO	eV	Ir	carbazole1	pyridine1	phenyl1	carbazole2	pyridine2	phenyl2	pic
L+5	-1.05	1	2	28	5	1	13	2	46
L+4	-1.1	2	2	38	6	3	42	6	2
L+3	-1.29	1	1	15	3	2	25	4	50
L+2	-1.7	5	6	53	16	1	13	4	2
L+1	-1.74	5	1	5	2	3	36	14	33
LUMO	-1.83	1	1	8	3	2	17	6	63
HOMO	-5.36	0	100	0	0	0	0	0	0
H-1	-5.37	0	0	0	0	100	0	0	0
H-2	-5.6	43	4	3	20	1	3	19	7
H-3	-5.7	28	48	11	1	1	1	2	8
H-4	-5.79	10	1	0	1	76	11	0	1
H-5	-6.07	28	36	6	6	0	1	2	20

Table S6: *Complex **4**, Geometry 2 - Frontier orbital energies and distributions*

MO	eV	Ir	carbazole1	pyridine1	phenyl1	carbazole2	pyridine2	phenyl2	pic
L+5	-1.04	1	2	26	5	1	14	3	47
L+4	-1.1	2	2	40	6	2	40	6	2
L+3	-1.29	1	1	14	2	2	26	5	49
L+2	-1.7	5	6	55	17	1	10	3	3
L+1	-1.74	5	0	4	1	4	39	14	32
LUMO	-1.82	1	1	8	3	2	17	6	63
HOMO	-5.36	0	100	0	0	0	0	0	0
H-1	-5.37	0	0	0	0	100	0	0	0
H-2	-5.6	44	3	3	20	1	3	19	7
H-3	-5.7	27	48	11	1	2	1	2	9
H-4	-5.79	11	2	1	1	74	11	0	1
H-5	-6.07	28	35	6	6	1	1	2	20

Table S7: *Complex **4**, Geometry 3 - Frontier orbital energies and distributions*

MO	eV	Ir	carbazole1	pyridine1	phenyl1	carbazole2	pyridine2	phenyl2	pic
L+5	-1.04	1	2	26	5	1	15	3	48
L+4	-1.1	2	2	40	6	2	39	6	2
L+3	-1.29	1	1	14	3	2	26	5	49
L+2	-1.7	4	6	57	17	1	7	2	5
L+1	-1.74	5	0	2	1	4	43	16	29
LUMO	-1.82	1	1	8	3	1	15	6	64
HOMO	-5.36	0	100	0	0	0	0	0	0
H-1	-5.37	0	0	0	0	100	0	0	0
H-2	-5.6	44	3	3	20	1	3	19	7
H-3	-5.7	26	51	11	1	0	1	2	9
H-4	-5.79	10	0	0	1	76	12	0	1
H-5	-6.07	29	35	6	6	0	1	2	20

Table S8: *Complex **4**, Geometry 4 - Frontier orbital energies and distributions*

MO	eV	Ir	carbazole1	pyridine1	phenyl1	carbazole2	pyridine2	phenyl2	pic
L+5	-1.04	1	1	14	2	2	27	5	46
L+4	-1.09	2	3	42	6	2	38	6	2
L+3	-1.29	1	2	24	4	1	15	3	51
L+2	-1.7	5	1	12	4	6	54	17	2
L+1	-1.73	5	4	38	14	1	5	2	30
LUMO	-1.83	1	1	15	6	1	7	3	66
HOMO	-5.36	0	0	0	0	100	0	0	0
H-1	-5.38	0	100	0	0	0	0	0	0
H-2	-5.6	43	1	3	19	3	3	20	7
H-3	-5.69	27	3	1	2	46	10	1	9
H-4	-5.79	11	72	11	0	3	1	1	1
H-5	-6.07	28	1	1	2	36	6	7	20

Table S9: *Complex **5**, Geometry 1 - Frontier orbital energies and distributions*

MO	eV	Ir	carbazole1	pyridine1	phenyl1	carbazole2	pyridine2	phenyl2	pic
L+5	-1.19	1	2	19	4	1	13	2	58
L+4	-1.27	2	3	43	6	2	37	5	1
L+3	-1.44	1	1	18	3	2	30	5	40
L+2	-1.9	4	5	48	17	1	6	2	17
L+1	-1.92	4	0	2	1	2	23	10	57
LUMO	-2.01	2	1	14	7	3	34	15	24
HOMO	-5.4	0	100	0	0	0	0	0	0
H-1	-5.4	0	0	0	0	100	0	0	0
H-2	-5.82	14	65	10	0	4	1	1	5
H-3	-5.88	6	4	1	0	78	11	0	1
H-4	-6.13	51	0	4	15	0	4	15	11
H-5	-6.27	37	20	5	4	0	2	3	29

Table S10: *Complex **5**, Geometry 2 - Frontier orbital energies and distributions*

MO	eV	Ir	carbazole1	pyridine1	phenyl1	carbazole2	pyridine2	phenyl2	pic
L+5	-1.19	1	1	18	4	1	14	2	58
L+4	-1.27	2	3	45	7	2	35	5	1
L+3	-1.44	1	1	17	3	2	31	5	40
L+2	-1.9	4	4	41	15	0	1	0	34
L+1	-1.92	4	1	9	3	3	27	11	41
LUMO	-2	2	1	14	6	3	34	15	24
HOMO	-5.4	0	100	0	0	0	0	0	0
H-1	-5.41	0	0	0	0	100	0	0	0
H-2	-5.82	14	67	11	0	1	1	1	5
H-3	-5.87	6	2	0	0	80	11	0	1
H-4	-6.12	51	0	4	15	0	4	15	11
H-5	-6.27	37	20	5	4	1	1	3	29

Table S11: *Complex **5**, Geometry 3 - Frontier orbital energies and distributions*

MO	eV	Ir	carbazole1	pyridine1	phenyl1	carbazole2	pyridine2	phenyl2	pic
L+5	-1.19	1	1	17	4	1	14	2	59
L+4	-1.27	2	3	46	7	2	35	5	1
L+3	-1.44	1	1	17	3	2	31	5	39
L+2	-1.89	4	4	39	14	0	1	0	38
L+1	-1.92	4	1	12	4	3	27	11	38
LUMO	-2.00	2	1	14	7	3	35	16	22
HOMO	-5.39	0	100	0	0	0	0	0	0
H-1	-5.41	0	0	0	0	100	0	0	0
H-2	-5.82	13	69	11	0	0	0	1	5
H-3	-5.88	6	0	0	0	81	11	0	1
H-4	-6.12	51	0	4	15	0	3	15	11
H-5	-6.27	37	19	5	4	0	2	3	29

Table S12: *Complex **5**, Geometry 4 - Frontier orbital energies and distributions*

MO	eV	Ir	carbazole1	pyridine1	phenyl1	carbazole2	pyridine2	phenyl2	pic
L+5	-1.19	1	2	19	4	1	14	2	57
L+4	-1.27	2	3	43	6	3	37	6	1
L+3	-1.44	1	1	18	3	2	29	5	41
L+2	-1.90	4	5	46	17	0	2	1	25
L+1	-1.91	5	1	5	2	3	29	12	45
LUMO	-2.00	2	1	13	6	3	32	14	29
HOMO	-5.40	0	100	0	0	0	0	0	0
H-1	-5.41	0	0	0	0	100	0	0	0
H-2	-5.82	15	64	10	0	3	1	1	5
H-3	-5.88	6	4	1	0	77	11	0	1
H-4	-6.12	51	0	4	15	0	4	15	11
H-5	-6.27	36	21	5	4	0	1	3	28

Table S13: *Complex **6**, Geometry 1 - Frontier orbital energies and distributions*

MO	eV	Ir	carbazole1	pyridine1	phenyl1	carbazole2	pyridine2	phenyl2	pic
L+5	-1.27	2	0	3	16	0	3	67	8
L+4	-1.35	2	2	42	6	3	36	8	0
L+3	-1.52	1	1	19	5	2	31	9	32
L+2	-1.96	4	2	21	8	0	0	0	65
L+1	-1.99	4	3	27	11	2	23	10	21
LUMO	-2.08	3	1	15	8	3	38	19	13
HOMO	-5.42	0	100	0	0	0	0	0	0
H-1	-5.43	0	0	0	0	100	0	0	0
H-2	-5.86	13	66	10	1	5	1	1	4
H-3	-5.91	6	5	1	0	78	10	0	1
H-4	-6.03	44	1	3	20	1	3	20	8
H-5	-6.33	38	18	6	3	0	1	2	31

Table S14: Complex **6**, Geometry 2 - *Frontier orbital energies and distributions*

MO	eV	Ir	carbazole1	pyridine1	phenyl1	carbazole2	pyridine2	phenyl2	pic
L+5	-1.27	2	0	3	16	0	3	68	8
L+4	-1.35	2	3	43	7	3	36	8	0
L+3	-1.52	1	1	19	5	2	31	9	32
L+2	-1.96	4	2	14	5	0	0	0	74
L+1	-1.99	4	3	33	13	2	23	10	11
LUMO	-2.08	3	1	15	8	3	37	19	13
HOMO	-5.42	0	100	0	0	0	0	0	0
H-1	-5.43	0	0	0	0	100	0	0	0
H-2	-5.86	13	70	10	1	1	0	1	5
H-3	-5.91	6	1	0	1	80	10	1	1
H-4	-6.03	43	1	3	20	2	3	20	8
H-5	-6.33	38	18	6	3	1	1	3	31

Table S15: Complex **6**, Geometry 3 - *Frontier orbital energies and distributions*

MO	eV	Ir	carbazole1	pyridine1	phenyl1	carbazole2	pyridine2	phenyl2	pic
L+5	-1.27	2	0	4	15	0	3	67	7
L+4	-1.34	2	3	43	7	3	35	8	0
L+3	-1.52	1	1	18	5	2	32	9	31
L+2	-1.95	4	2	19	7	0	0	0	68
L+1	-1.99	4	3	30	12	2	21	9	19
LUMO	-2.08	3	1	13	7	4	40	20	12
HOMO	-5.42	0	100	0	0	0	0	0	0
H-1	-5.43	0	0	0	0	100	0	0	0
H-2	-5.86	12	70	10	1	1	0	1	4
H-3	-5.92	6	1	0	1	80	11	0	1
H-4	-6.02	44	1	3	20	1	3	20	8
H-5	-6.33	38	18	5	3	0	1	3	31

Table S16: Complex **6**, Geometry 4 - *Frontier orbital energies and distributions*

MO	eV	Ir	carbazole1	pyridine1	phenyl1	carbazole2	pyridine2	phenyl2	pic
L+5	-1.27	2	0	4	16	0	3	68	7
L+4	-1.35	2	2	42	6	3	37	8	0
L+3	-1.52	1	1	20	5	2	30	9	32
L+2	-1.96	4	2	17	6	0	0	0	70
L+1	-1.99	4	3	30	12	2	24	10	13
LUMO	-2.08	2	1	15	8	3	36	18	15
HOMO	-5.42	0	100	0	0	0	0	0	0
H-1	-5.43	0	0	0	0	100	0	0	0
H-2	-5.86	13	67	10	1	3	1	1	5
H-3	-5.92	7	3	0	1	77	10	1	1
H-4	-6.03	43	1	3	20	2	4	20	7
H-5	-6.33	38	19	6	3	0	1	3	30

TD-DFT calculations

Table S17: TD-DFT calculations showing the energy and composition of excited states T_1-T_5 for complex **2**. Calculations were conducted at the optimised S_0 geometry. Electron density transfer to/from key groups is shown (%).

No.	wavelength (nm)	major contributions	Ir	mesityl1	pyridine1	phenyl1	mesityl2	pyridine2	phenyl2	picolinate
1	413.3771	H-7->L+2 (13%), H-1->L+2 (17%), HOMO->LUMO (12%), HOMO->L+2 (25%)	42-->4 (-38)	1-->1 (0)	9-->39 (30)	19-->16 (-3)	0-->0 (0)	3-->15 (12)	9-->7 (-2)	17-->18 (1)
2	406.9191	H-2->L+1 (14%), HOMO->L+1 (16%), HOMO->L+2 (11%)	42-->4 (-38)	2-->0 (-2)	4-->15 (11)	8-->6 (-2)	7-->1 (-6)	10-->29 (19)	17-->13 (-4)	10-->33 (23)
3	406.5855	H-1->LUMO (45%), H-1->L+1 (21%)	49-->3 (-46)	0-->0 (0)	6-->7 (1)	6-->3 (-3)	0-->1 (1)	2-->22 (20)	8-->11 (3)	28-->53 (25)
4	378.9132	H-1->LUMO (11%), HOMO->LUMO (41%), HOMO->L+1 (23%)	45-->3 (-42)	0-->0 (0)	5-->7 (2)	12-->3 (-9)	0-->1 (1)	3-->22 (19)	11-->11 (0)	23-->54 (31)
5	375.4253	H-1->L+2 (46%), HOMO->L+2 (24%)	49-->4 (-45)	0-->1 (1)	7-->44 (37)	8-->18 (10)	0-->0 (0)	3-->15 (12)	8-->6 (-2)	25-->11 (-14)

Table S18: TD-DFT calculations showing the energy and composition of excited states T_1-T_5 for complex **3**. Calculations were conducted at the optimised S_0 geometry. Electron density transfer to/from key groups is shown (%).

No.	wavelength (nm)	major contributions	Ir	mesityl1	pyridine1	phenyl1	mesityl2	pyridine2	phenyl2	picolinate
1	423.5011	HOMO->LUMO (41%), HOMO->L+1 (13%)	39-->3 (-36)	0-->1 (1)	5-->20 (15)	20-->10 (-10)	0-->1 (1)	4-->23 (19)	19-->12 (-7)	13-->31 (18)
2	418.0464	HOMO->L+2 (33%)	40-->4 (-36)	2-->1 (-1)	5-->35 (30)	18-->18 (0)	0-->0 (0)	4-->16 (12)	16-->8 (-8)	15-->18 (3)
3	403.8047	H-1->LUMO (25%), H-1->L+1 (52%)	52-->4 (-48)	0-->0 (0)	8-->7 (-1)	2-->4 (2)	0-->1 (1)	2-->23 (21)	3-->13 (10)	33-->49 (16)
4	389.4587	H-1->LUMO (17%), H-1->L+2 (34%), HOMO->L+2 (31%)	48-->4 (-44)	0-->1 (1)	6-->40 (34)	11-->19 (8)	0-->0 (0)	2-->16 (14)	11-->8 (-3)	22-->13 (-9)
5	385.6549	HOMO->LUMO (23%), HOMO->L+1 (56%)	42-->4 (-38)	0-->0 (0)	4-->7 (3)	21-->4 (-17)	0-->1 (1)	3-->23 (20)	20-->12 (-8)	10-->49 (39)

Table S19: TD-DFT calculations showing the energy and composition of excited states T_1-T_5 for complex **4**, geometry 1. Calculations were conducted at the optimised S_0 geometry. Electron density transfer to/from key groups is shown (%).

No.	wavelength (nm)	major contributions	Ir	carbazole1	pyridine1	phenyl1	carbazole2	pyridine2	phenyl2	picolinate
1	442.1533	H-3->L+2 (28%), H-2->LUMO (12%), H-2->L+1 (12%)	32-->4 (-28)	29-->3 (-26)	8-->30 (22)	11-->9 (-2)	1-->2 (1)	2-->19 (17)	9-->7 (-2)	8-->26 (18)
2	437.2106	H-4->L+1 (10%), H-3->L+2 (19%), H-2->L+1 (18%), H-2->L+2 (10%)	32-->4 (-28)	14-->2 (-12)	5-->23 (18)	11-->7 (-4)	16-->2 (-14)	5-->24 (19)	13-->9 (-4)	6-->28 (22)
3	419.2621	H-5->LUMO (17%), H-5->L+1 (11%), H-3->LUMO (24%), H-3->L+1 (21%)	29-->3 (-26)	40-->1 (-39)	9-->13 (4)	5-->5 (0)	1-->2 (1)	1-->23 (22)	4-->9 (5)	12-->44 (32)
4	417.399	H-3->LUMO (10%), H-2->LUMO (20%), H-2->L+2 (46%)	39-->3 (-36)	14-->4 (-10)	5-->36 (31)	16-->11 (-5)	1-->1 (0)	2-->14 (12)	15-->5 (-10)	8-->25 (17)
5	413.0466	H-2->LUMO (44%), H-2->L+1 (41%)	43-->3 (-40)	4-->1 (-3)	3-->10 (7)	20-->4 (-16)	1-->2 (1)	3-->25 (22)	19-->9 (-10)	7-->45 (38)

Table S20: TD-DFT calculations showing the energy and composition of excited states T_1-T_5 for complex **4**, geometry 2. Calculations were conducted at the optimised S_0 geometry. Electron density transfer to/from key groups is shown (%).

No.	Wavelength (nm)	Major contributions	Ir	carbazole1	pyridine1	phenyl1	carbazole2	pyridine2	phenyl2	picolinate
1	442.106	H-3->L+2 (34%), H-2->LUMO (12%), H-2->L+1 (10%)	31-->4 (-27)	28-->4 (-24)	8-->35 (27)	10-->11 (1)	4-->2 (-2)	2-->17 (15)	8-->6 (-2)	9-->22 (13)
2	437.2723	H-4->L+1 (11%), H-3->L+2 (10%), H-2->L+1 (22%)	32-->4 (-28)	8-->2 (-6)	4-->20 (16)	12-->6 (-6)	19-->3 (-16)	6-->26 (20)	14-->9 (-5)	6-->30 (24)
3	419.7163	H-5->LUMO (16%), H-5->L+1 (10%), H-3->LUMO (24%), H-3->L+1 (21%)	29-->3 (-26)	39-->1 (-38)	8-->13 (5)	5-->5 (0)	2-->2 (0)	1-->24 (23)	4-->9 (5)	12-->43 (31)
4	417.399	H-3->LUMO (11%), H-3->L+2 (11%), H-2->LUMO (14%), H-2->L+2 (49%)	39-->3 (-36)	16-->4 (-12)	5-->40 (35)	15-->13 (-2)	1-->1 (0)	2-->12 (10)	14-->4 (-10)	8-->22 (14)
5	412.8953	H-2->LUMO (42%), H-2->L+1 (43%)	44-->3 (-41)	3-->1 (-2)	3-->9 (6)	20-->3 (-17)	1-->3 (2)	3-->27 (24)	19-->10 (-9)	7-->45 (38)

Table S21: TD-DFT calculations showing the energy and composition of excited states T_1-T_5 for complex **4**, geometry 3. Calculations were conducted at the optimised S_0 geometry. Electron density transfer to/from key groups is shown (%).

No.	wavelength (nm)	major contributions	Ir	carbazole1	pyridine1	phenyl1	carbazole2	pyridine2	phenyl2	picolinate
1	441.8066	H-3->L+2 (31%), H-2->LUMO (13%), H-2->L+1 (11%)	31-->4 (-27)	28-->4 (-24)	8-->34 (26)	11-->11 (0)	3-->2 (-1)	2-->16 (14)	9-->6 (-3)	8-->24 (16)
2	437.3032	H-4->L+1 (11%), H-3->L+2 (15%), H-2->L+1 (25%)	32-->4 (-28)	11-->2 (-9)	4-->19 (15)	12-->6 (-6)	15-->3 (-12)	5-->28 (23)	14-->10 (-4)	6-->28 (22)
3	418.8797	H-5->LUMO (15%), H-3->LUMO (20%), H-3->L+1 (18%)	30-->3 (-27)	39-->2 (-37)	8-->17 (9)	6-->6 (0)	0-->2 (2)	1-->22 (21)	5-->8 (3)	12-->40 (28)
4	416.9919	H-3->LUMO (15%), H-2->LUMO (17%), H-2->L+2 (42%)	38-->3 (-35)	18-->4 (-14)	5-->36 (31)	14-->11 (-3)	0-->1 (1)	2-->11 (9)	14-->4 (-10)	8-->30 (22)
5	412.8265	H-2->LUMO (40%), H-2->L+1 (37%), H-2->L+2 (13%)	44-->3 (-41)	3-->1 (-2)	3-->13 (10)	20-->4 (-16)	1-->3 (2)	3-->25 (22)	19-->9 (-10)	7-->41 (34)

Table S22: TD-DFT calculations showing the energy and composition of excited states T_1-T_5 for complex **4**, geometry 4. Calculations were conducted at the optimised S_0 geometry. Electron density transfer to/from key groups is shown (%).

No.	wavelength (nm)	major contributions	Ir	carbazole1	pyridine1	phenyl1	carbazole2	pyridine2	phenyl2	picolinate
1	441.7437	H-3->L+2 (36%)	30-->4 (-26)	5-->2 (-3)	2-->18 (16)	8-->6 (-2)	29-->4 (-25)	8-->35 (27)	9-->11 (2)	9-->20 (11)
2	436.9025	H-4->L+1 (11%), H-2->L+1 (23%)	32-->4 (-28)	20-->3 (-17)	6-->26 (20)	14-->10 (-4)	7-->2 (-5)	3-->19 (16)	12-->6 (-6)	5-->30 (25)
3	420.2427	H-5->LUMO (18%), H-5->L+1 (10%), H-3->LUMO (30%), H-3->L+1 (20%)	28-->3 (-25)	2-->2 (0)	1-->23 (22)	3-->8 (5)	40-->1 (-39)	9-->11 (2)	4-->4 (0)	12-->48 (36)
4	417.4552	H-3->L+2 (11%), H-2->LUMO (18%), H-2->L+2 (53%)	40-->4 (-36)	1-->1 (0)	2-->13 (11)	16-->4 (-12)	12-->4 (-8)	4-->41 (37)	17-->13 (-4)	8-->20 (12)
5	413.0879	H-2->LUMO (49%), H-2->L+1 (35%)	43-->3 (-40)	1-->2 (1)	3-->24 (21)	19-->9 (-10)	3-->1 (-2)	3-->10 (7)	20-->4 (-16)	7-->47 (40)

Table S23: TD-DFT calculations showing the energy and composition of excited states T_1-T_5 for complex **5**, geometry 1. Calculations were conducted at the optimised S_0 geometry. Electron density transfer to/from key groups is shown (%).

No.	wavelength (nm)	major contributions	Ir	carbazole1	pyridine1	phenyl1	carbazole2	pyridine2	phenyl2	picolinate
1	436.6102	H-2->LUMO (19%), H-2->L+2 (47%)	18-->4 (-14)	55-->4 (-51)	10-->39 (29)	4-->14 (10)	3-->1 (-2)	1-->13 (12)	2-->5 (3)	7-->19 (12)
2	430.2019	H-1->LUMO (62%), H-1->L+1 (22%)	0-->3 (3)	0-->1 (1)	0-->13 (13)	0-->6 (6)	100-->8 (-92)	0-->28 (28)	0-->12 (12)	0-->30 (30)
3	429.1595	H-3->LUMO (35%), H-3->L+1 (20%)	16-->3 (-13)	3-->1 (-2)	1-->12 (11)	2-->5 (3)	61-->3 (-58)	10-->28 (18)	4-->12 (8)	3-->35 (32)
4	427.4285	HOMO->LUMO (34%), HOMO->L+2 (52%)	0-->3 (3)	100-->10 (-90)	0-->31 (31)	0-->12 (12)	0-->1 (1)	0-->16 (16)	0-->7 (7)	0-->19 (19)
5	409.7703	H-5->LUMO (10%), H-5->L+1 (27%), H-2->L+1 (21%)	28-->4 (-24)	38-->1 (-37)	7-->12 (5)	3-->5 (2)	2-->2 (0)	1-->23 (22)	3-->10 (7)	18-->43 (25)

Table S24: TD-DFT calculations showing the energy and composition of excited states T_1-T_5 for complex **5**, geometry 2. Calculations were conducted at the optimised S_0 geometry. Electron density transfer to/from key groups is shown (%).

No.	wavelength (nm)	major contributions	Ir	carbazole1	pyridine1	phenyl1	carbazole2	pyridine2	phenyl2	picolinate
1	436.6102	H-2->LUMO (17%), H-2->L+2 (43%)	17-->4 (-13)	58-->3 (-55)	10-->31 (21)	3-->12 (9)	1-->1 (0)	1-->12 (11)	2-->5 (3)	7-->32 (25)
2	429.8738	H-1->LUMO (57%), H-1->L+1 (25%)	0-->3 (3)	0-->1 (1)	0-->12 (12)	0-->5 (5)	99-->8 (-91)	0-->30 (30)	0-->13 (13)	0-->27 (27)
3	428.9368	H-3->LUMO (32%), H-3->L+1 (22%)	15-->3 (-12)	1-->1 (0)	1-->12 (11)	2-->5 (3)	65-->3 (-62)	9-->31 (22)	4-->14 (10)	2-->31 (29)
4	427.1929	HOMO->LUMO (31%), HOMO->L+1 (11%), HOMO->L+2 (47%)	0-->3 (3)	100-->10 (-90)	0-->26 (26)	0-->10 (10)	0-->1 (1)	0-->15 (15)	0-->6 (6)	0-->29 (29)
5	410.1634	H-5->LUMO (10%), H-5->L+1 (19%), H-5->L+2 (15%), H-2->L+1 (16%), H-2->L+2 (12%)	27-->4 (-23)	41-->2 (-39)	8-->21 (13)	3-->8 (5)	1-->2 (1)	1-->21 (20)	3-->9 (6)	18-->35 (17)

Table S25: TD-DFT calculations showing the energy and composition of excited states T_1-T_5 for complex **5**, geometry 3. Calculations were conducted at the optimised S_0 geometry. Electron density transfer to/from key groups is shown (%).

No.	wavelength (nm)	major contributions	Ir	carbazole1	pyridine1	phenyl1	carbazole2	pyridine2	phenyl2	picolinate
1	436.3643	H-2->LUMO (18%), H-2->L+1 (10%), H-2->L+2 (40%)	17-->4 (-13)	60-->3 (-57)	10-->29 (19)	3-->11 (8)	0-->1 (1)	1-->13 (12)	2-->6 (4)	7-->34 (27)
2	429.6205	H-1->LUMO (62%), H-1->L+1 (27%)	0-->3 (3)	0-->1 (1)	0-->13 (13)	0-->6 (6)	100-->9 (-91)	0-->30 (30)	0-->13 (13)	0-->25 (25)
3	428.6995	H-3->LUMO (37%), H-3->L+1 (25%)	16-->3 (-13)	1-->1 (0)	1-->13 (12)	2-->6 (4)	63-->3 (-60)	10-->32 (22)	4-->14 (10)	2-->29 (27)
4	427.812	HOMO->LUMO (32%), HOMO->L+1 (15%), HOMO->L+2 (42%)	0-->3 (3)	100-->9 (-91)	0-->24 (24)	0-->9 (9)	0-->2 (2)	0-->16 (16)	0-->7 (7)	0-->30 (30)
5	409.432	H-5->L+1 (18%), H-5->L+2 (17%), H-2->L+1 (14%), H-2->L+2 (14%)	28-->4 (-24)	40-->2 (-38)	7-->22 (15)	3-->8 (5)	0-->2 (2)	1-->19 (18)	3-->8 (5)	18-->35 (17)

Table S26: TD-DFT calculations showing the energy and composition of excited states T_1-T_5 for complex **5**, geometry 4. Calculations were conducted at the optimised S_0 geometry. Electron density transfer to/from key groups is shown (%).

No.	wavelength (nm)	major contributions	Ir	carbazole1	pyridine1	phenyl1	carbazole2	pyridine2	phenyl2	picolinate
1	436.7178	H-2->LUMO (17%), H-2->L+2 (48%)	18-->4 (-14)	55-->4 (-51)	10-->36 (26)	4-->14 (10)	3-->1 (-2)	1-->10 (9)	2-->4 (2)	8-->27 (19)
2	428.9814	H-3->LUMO (17%), H-3->L+1 (13%), H-1->LUMO (26%), H-1->L+1 (13%)	9-->3 (-6)	1-->1 (0)	1-->10 (9)	1-->4 (3)	78-->6 (-72)	5-->30 (25)	2-->13 (11)	1-->34 (33)
3	428.3737	H-3->LUMO (14%), H-3->L+1 (11%), H-1->LUMO (32%), H-1->L+1 (15%)	6-->3 (-3)	1-->1 (0)	0-->10 (10)	1-->4 (3)	85-->7 (-78)	4-->29 (25)	2-->13 (11)	1-->33 (32)
4	426.7518	HOMO->LUMO (30%), HOMO->L+2 (52%)	0-->3 (3)	100-->11 (-89)	0-->30 (30)	0-->11 (11)	0-->1 (1)	0-->13 (13)	0-->6 (6)	0-->26 (26)
5	410.9519	H-5->LUMO (12%), H-5->L+1 (20%), H-5->L+2 (10%), H-2->LUMO (12%), H-2->L+1 (19%), H-2->L+2 (10%)	26-->4 (-22)	42-->2 (-40)	8-->17 (9)	2-->7 (5)	2-->2 (0)	1-->23 (22)	2-->10 (8)	17-->35 (18)

Table S27: TD-DFT calculations showing the energy and composition of excited states T_1-T_5 for complex **6**, geometry 1. Calculations were conducted at the optimised S_0 geometry. Electron density transfer to/from key groups is shown (%).

No.	wavelength (nm)	major contributions	Ir	carbazole1	pyridine1	phenyl1	carbazole2	pyridine2	phenyl2	picolinate
1	439.8474	H-2->LUMO (17%), H-2->L+1 (21%), H-2->L+2 (18%)	19-->4 (-15)	51-->2 (-49)	8-->21 (13)	5-->9 (4)	6-->2 (-4)	2-->21 (19)	5-->10 (5)	5-->31 (26)
2	438.3855	H-1->LUMO (71%), H-1->L+1 (22%)	0-->3 (3)	0-->2 (2)	0-->17 (17)	0-->8 (8)	100-->6 (-94)	0-->33 (33)	0-->16 (16)	0-->14 (14)
3	435.0017	HOMO->LUMO (37%), HOMO->L+1 (32%), HOMO->L+2 (22%)	0-->3 (3)	100-->6 (-94)	0-->20 (20)	0-->9 (9)	0-->2 (2)	0-->23 (23)	0-->11 (11)	0-->27 (27)
4	434.3769	H-4->LUMO (15%), H-3->LUMO (32%), H-3->L+1 (14%)	18-->3 (-15)	5-->2 (-3)	2-->19 (17)	7-->9 (2)	50-->3 (-47)	7-->33 (26)	7-->16 (9)	3-->15 (12)
5	413.4598	H-4->LUMO (43%), H-3->LUMO (16%), H-2->LUMO (13%)	28-->3 (-25)	11-->1 (-10)	4-->16 (12)	12-->9 (-3)	23-->3 (-20)	5-->34 (29)	12-->19 (7)	5-->15 (10)

Table S28: TD-DFT calculations showing the energy and composition of excited states T_1-T_5 for complex **6**, geometry 2. Calculations were conducted at the optimised S_0 geometry. Electron density transfer to/from key groups is shown (%).

No.	wavelength (nm)	major contributions	Ir	carbazole1	pyridine1	phenyl1	carbazole2	pyridine2	phenyl2	picolinate
1	440.2222	H-2->LUMO (17%), H-2->L+1 (30%), H-2->L+2 (14%)	19-->4 (-15)	56-->2 (-54)	9-->24 (15)	4-->10 (6)	1-->2 (1)	1-->23 (22)	4-->10 (6)	6-->25 (19)
2	437.72	H-1->LUMO (69%), H-1->L+1 (23%)	0-->3 (3)	0-->2 (2)	0-->19 (19)	0-->9 (9)	100-->6 (-94)	0-->33 (33)	0-->16 (16)	0-->12 (12)
3	435.0781	HOMO->LUMO (36%), HOMO->L+1 (41%), HOMO->L+2 (15%)	0-->3 (3)	100-->6 (-94)	0-->22 (22)	0-->9 (9)	0-->2 (2)	0-->24 (24)	0-->11 (11)	0-->21 (21)
4	434.0423	H-4->LUMO (18%), H-3->LUMO (28%), H-3->L+1 (15%)	19-->3 (-16)	4-->2 (-2)	2-->20 (18)	7-->9 (2)	49-->3 (-46)	7-->33 (26)	7-->16 (9)	3-->13 (10)
5	413.2669	H-4->LUMO (41%), H-3->LUMO (26%)	27-->3 (-24)	5-->2 (-3)	3-->17 (14)	11-->9 (-2)	32-->3 (-29)	6-->33 (27)	11-->19 (8)	5-->15 (10)

Table S29: TD-DFT calculations showing the energy and composition of excited states T_1-T_5 for complex **6**, geometry 3. Calculations were conducted at the optimised S_0 geometry. Electron density transfer to/from key groups is shown (%).

No.	wavelength (nm)	major contributions	Ir	carbazole1	pyridine1	phenyl1	carbazole2	pyridine2	phenyl2	picolinate
1	438.9909	H-2->LUMO (15%), H-2->L+1 (26%), H-2->L+2 (17%)	20-->4 (-16)	54-->2 (-52)	9-->22 (13)	5-->9 (4)	1-->2 (1)	1-->21 (20)	5-->10 (5)	6-->30 (24)
2	437.2723	H-1->LUMO (72%), H-1->L+1 (20%)	0-->3 (3)	0-->2 (2)	0-->16 (16)	0-->8 (8)	100-->7 (-93)	0-->34 (34)	0-->17 (17)	0-->13 (13)
3	434.2856	H-3->LUMO (13%), HOMO->LUMO (19%), HOMO->L+1 (23%), HOMO->L+2 (11%)	7-->3 (-4)	65-->5 (-60)	1-->20 (19)	3-->9 (6)	18-->2 (-16)	3-->26 (23)	3-->13 (10)	1-->21 (20)
4	434.0879	H-3->LUMO (19%), HOMO->LUMO (13%), HOMO->L+1 (16%)	10-->3 (-7)	49-->2 (-47)	1-->20 (19)	4-->9 (5)	27-->3 (-24)	4-->29 (25)	4-->14 (10)	2-->20 (18)
5	412.9228	H-4->LUMO (41%), H-3->LUMO (23%)	27-->3 (-24)	6-->1 (-5)	3-->15 (12)	11-->8 (-3)	30-->3 (-27)	6-->35 (29)	11-->20 (9)	5-->14 (9)

Table S30: TD-DFT calculations showing the energy and composition of excited states T_1-T_5 for complex **6**, geometry 4. Calculations were conducted at the optimised S_0 geometry. Electron density transfer to/from key groups is shown (%).

No.	wavelength (nm)	major contributions	Ir	carbazole1	pyridine1	phenyl1	carbazole2	pyridine2	phenyl2	picolinate
1	440.1441	H-2->LUMO (17%), H-2->L+1 (27%), H-2->L+2 (16%)	19-->4 (-15)	54-->2 (-52)	9-->22 (13)	4-->9 (5)	2-->2 (0)	1-->22 (21)	4-->10 (6)	6-->28 (22)
2	436.5026	H-1->LUMO (66%), H-1->L+1 (24%)	0-->3 (3)	0-->2 (2)	0-->19 (19)	0-->9 (9)	100-->7 (-93)	0-->31 (31)	0-->15 (15)	0-->14 (14)
3	434.7577	HOMO->LUMO (36%), HOMO->L+1 (38%), HOMO->L+2 (17%)	0-->3 (3)	100-->6 (-94)	0-->21 (21)	0-->9 (9)	0-->2 (2)	0-->23 (23)	0-->11 (11)	0-->24 (24)
4	433.6021	H-4->LUMO (17%), H-3->LUMO (24%), H-3->L+1 (15%)	20-->3 (-17)	8-->2 (-6)	2-->20 (18)	8-->9 (1)	44-->3 (-41)	7-->32 (25)	8-->16 (8)	4-->15 (11)
5	412.6067	H-4->LUMO (39%), H-3->LUMO (27%)	27-->3 (-24)	5-->2 (-3)	3-->17 (14)	11-->9 (-2)	32-->3 (-29)	6-->31 (25)	11-->18 (7)	5-->17 (12)

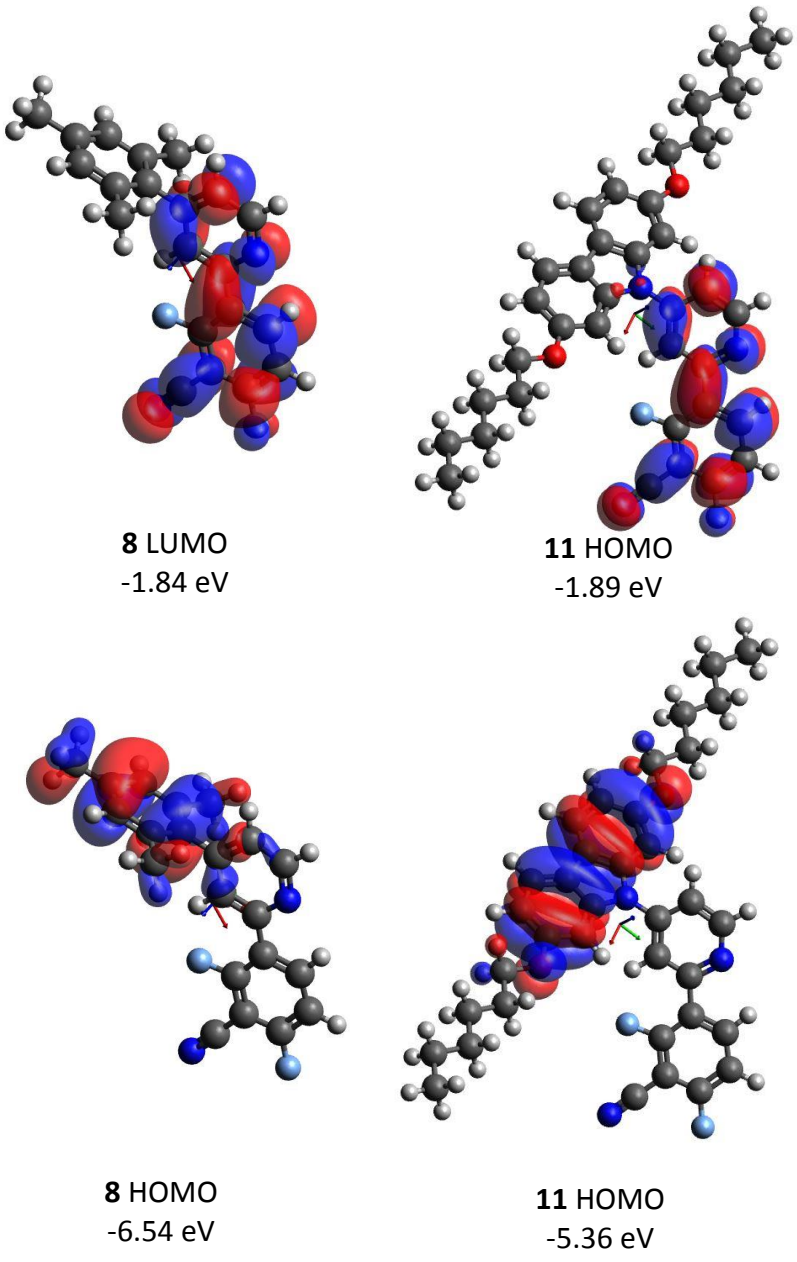

Figure S26: Frontier molecular orbitals for **8** and **11**. Isocontour set to 0.02000.

Table S31: TD-DFT calculations showing the energy and composition of excited states S_1-S_{10} for ligand **9**. Calculations were conducted at the optimised S_0 geometry. Electron density transfer to/from key groups is shown (%).

No.	Wavelength (nm)	Osc. Strength	Major contributions	carbazole	pyridine	phenyl
1	368.0257	0.0009	HOMO->LUMO (99%)	100-->3 (-97)	0-->57 (57)	0-->40 (40)
2	336.4382	0.0958	H-1->LUMO (98%)	89-->3 (-86)	11-->57 (46)	0-->40 (40)
3	315.3049	0.0001	HOMO->L+1 (99%)	100-->9 (-91)	0-->80 (80)	0-->12 (12)
4	294.8354	0.1585	H-1->L+1 (95%)	89-->9 (-80)	11-->80 (69)	0-->12 (12)
5	288.2549	0.6374	HOMO->L+2 (92%)	99-->99 (0)	1-->1 (0)	0-->0 (0)
6	286.1988	0.0014	H-1->L+2 (70%), HOMO->L+4 (24%)	92-->97 (5)	8-->2 (-6)	0-->0 (0)
7	278.0476	0.0026	H-5->LUMO (11%), H-4->LUMO (87%)	26-->3 (-23)	71-->57 (-14)	3-->40 (37)
8	267.7787	0.0031	HOMO->L+3 (99%)	100-->2 (-98)	0-->7 (7)	0-->91 (91)
9	266.5295	0.5571	H-2->LUMO (82%)	3-->4 (1)	36-->58 (22)	61-->38 (-23)
10	262.7674	0.0055	H-3->LUMO (95%)	100-->6 (-94)	0-->55 (55)	0-->39 (39)

Table S32: TD-DFT calculations showing the energy and composition of excited states S_1-S_{10} for ligand **10**. Calculations were conducted at the optimised S_0 geometry. Electron density transfer to/from key groups is shown (%).

No.	Wavelength (nm)	Osc. Strength	major contributions	carbazole	pyridine	phenyl
1	392.0945	0.0007	HOMO->LUMO (99%)	100-->3 (-97)	0-->49 (49)	0-->48 (48)
2	353.4629	0.0754	H-1->LUMO (98%)	89-->3 (-86)	11-->49 (38)	0-->48 (48)
3	325.1277	0.0005	HOMO->L+1 (90%)	100-->4 (-96)	0-->49 (49)	0-->47 (47)
4	301.0933	0.1438	H-1->L+1 (85%), H-1->L+2 (12%)	89-->5 (-84)	11-->48 (37)	0-->47 (47)
5	300.2766	0.0042	HOMO->L+1 (10%), HOMO->L+2 (88%)	100-->7 (-93)	0-->40 (40)	0-->53 (53)
6	288.1544	0.6462	HOMO->L+3 (92%)	99-->99 (0)	1-->1 (0)	0-->0 (0)
7	285.6581	0.0033	H-1->L+3 (69%), HOMO->L+4 (25%)	92-->97 (5)	8-->2 (-6)	0-->1 (1)
8	282.4306	0.0019	H-5->LUMO (39%), H-4->LUMO (58%)	50-->3 (-47)	47-->49 (2)	2-->48 (46)
9	276.9359	0.0687	H-1->L+1 (12%), H-1->L+2 (83%)	87-->6 (-81)	12-->41 (29)	2-->53 (51)
10	274.8181	0.0098	H-2->LUMO (96%)	100-->3 (-97)	0-->49 (49)	0-->48 (48)

Table S33: TD-DFT calculations showing the energy and composition of excited states S_1-S_{10} for ligand **11**. Calculations were conducted at the optimised S_0 geometry. Electron density transfer to/from key groups is shown (%).

No.	Wavelength (nm)	Osc. Strength	Major contributions	carbazole	pyridine	phenyl
1	405.7074	0.0006	HOMO->LUMO (98%)	100-->2 (-98)	0-->30 (30)	0-->68 (68)
2	362.2938	0.0631	H-1->LUMO (96%)	89-->2 (-87)	11-->30 (19)	0-->68 (68)
3	353.4629	0.0002	HOMO->L+1 (98%)	100-->1 (-99)	0-->25 (25)	0-->74 (74)
4	323.0269	0.0008	HOMO->L+2 (99%)	100-->11 (-89)	0-->83 (83)	0-->6 (6)
5	320.9614	0.0013	H-1->L+1 (95%)	89-->1 (-88)	11-->25 (14)	0-->74 (74)
6	298.2612	0.2113	H-1->L+2 (95%)	89-->11 (-78)	11-->83 (72)	0-->6 (6)
7	288.2683	0.6514	HOMO->L+3 (92%)	99-->99 (0)	1-->1 (0)	0-->0 (0)
8	285.5594	0.0004	H-2->LUMO (11%), H-1->L+3 (62%), HOMO->L+4 (22%)	93-->88 (-5)	7-->4 (-3)	0-->8 (8)
9	284.511	0.0009	H-5->LUMO (43%), H-4->LUMO (45%)	50-->2 (-48)	47-->30 (-17)	3-->69 (66)
10	281.3219	0.0057	H-2->LUMO (86%)	99-->13 (-86)	1-->27 (26)	0-->60 (60)

Device Fabrication

Devices were fabricated on glass substrates coated with a 125 nm layer of indium tin oxide (ITO) with a sheet resistance of 15 Ω/□ (VisionTek). Substrates were cleaned thoroughly in acetone and isopropyl alcohol (IPA) before undergoing ozone treatment for 5 min. A ca. 75 nm layer of poly(3,4-ethylenedioxythiophene):poly(styrenesulfonate) (PEDOT:PSS, Heraeus Clevios HIL 1.5) was spin coated at 2500 rpm for 1 min and then annealed at 200 °C for 3 min to remove water. The host material poly(vinylcarbazole) (PVK) was doped with 1,3-bis[(4-*tert*-butylphenyl)-1,3,4-oxadiazolyl]phenylene (OXD-7) and with the emissive iridium complex, blended in the ratio 100:50:8 (PVK:OXD-7:Ir) by weight in chlorobenzene solution at a concentration of 20 mg/mL PVK. The emissive layer was spin coated at 2500 rpm for 1 min and annealed at 120 °C for 10 min resulting in a film thickness of 76 ± 1 nm. TPBi and LiF/Al layers were thermally evaporated using the Kurt J. Lesker Spectros II deposition system operating at 1 x 10^{-6} mbar. Devices were encapsulated using UV curable epoxy (DELO KATIOBOND) and a glass cover slide, exposing to UV light for 3 min. Patterning of the ITO substrate combined with masking of the cathode produced four identical pixels of 5 mm x 4 mm for each device. The resulting structure of each device was ITO / PEDOT:PSS (50 nm) / PVK:OXD-7:Ir (75 nm) TPBi (25 nm)/LiF (1 nm)/Al. Current-voltage data, device efficiency, brightness and electroluminescence spectra were measured in a calibrated Labsphere LMS-100 integrating sphere. A home-written NI LabVIEW programme was used to control an Agilent 6632B DC power supply, and the emission properties of the device were measured using an Ocean Optics USB4000 CCD fibre optic spectrometer. Thicknesses of PVK:OXD-7:Ir layers were measured with a J A Woolam VASE Ellipsometer using thin films which had been spin coated on Si/SiO_2 substrates under the same conditions as the device films.

Thin Film measurements (zeonex)

Films of complex **5** doped in zeonex were fabricated as follows:
1) A solution of 100 mg/ml of zeonex in toluene was made
2) A solution of **5** in toluene was made at a concentration of 1 mg/5 ml.
3) The two solutions were mixed in a 1:1 v/v ratio and the resultant solution was spin-coated onto quartz substrates.

For decay measurements the substrates were mounted in a displex cryostat and evacuated with a turbomolecular pump. Samples were excited with a 450 nm dye laser pumped by a pulsed YAG laser emitting at 355 nm (from EKSPLA) at 45° angle to the substrate plane; the energy of each pulse was ca. 40 μJ per pulse. Emission was focused onto a spectrograph and detected on a sensitive gated iCCD camera (Stanford Computer Optics) with sub nanosecond resolution.

Copies of NMR spectra:

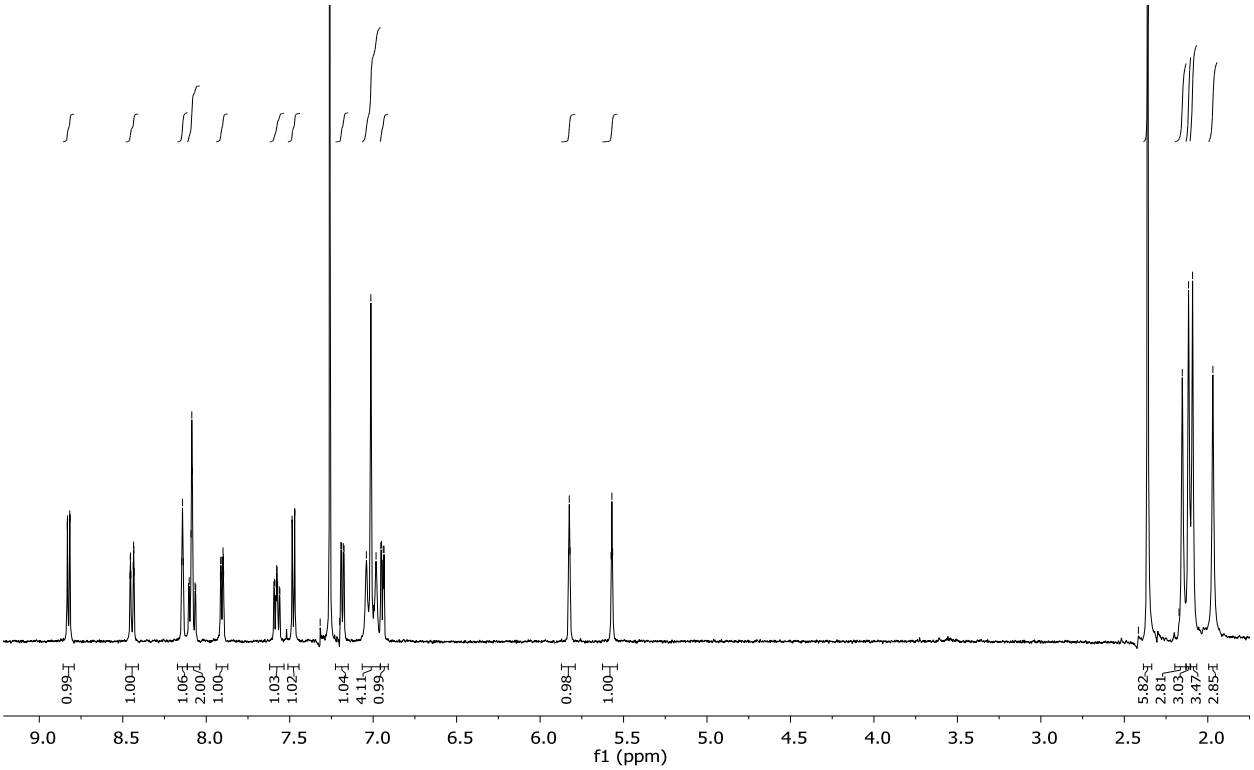

Figure S27: ^{1}H NMR spectrum of **2** in $CDCl_3$.

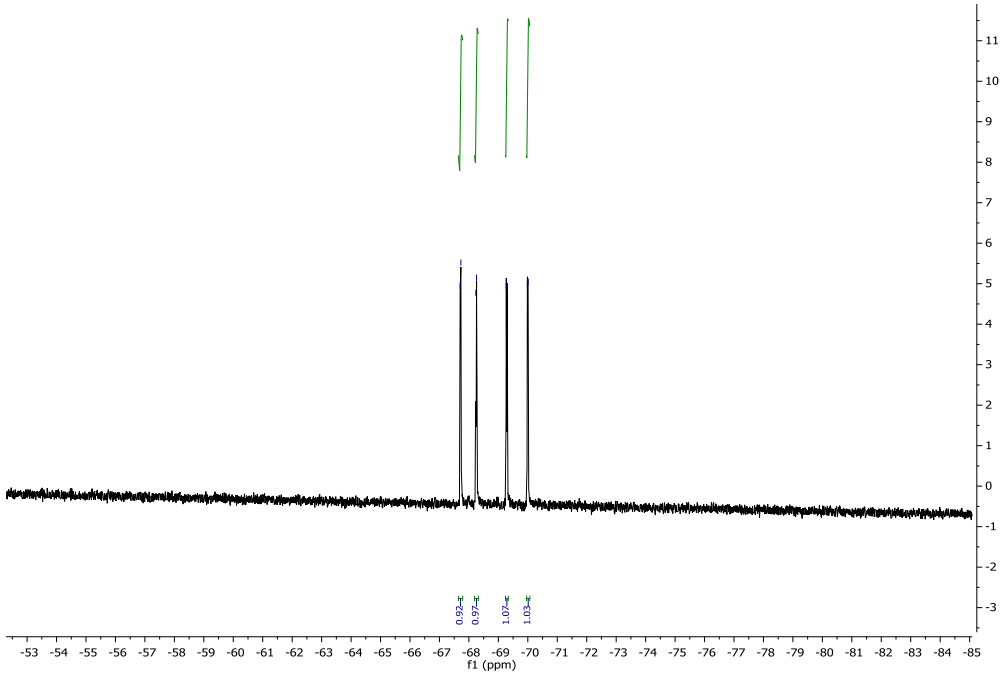

Figure S28: ^{19}F NMR spectrum of **2** in $CDCl_3$.

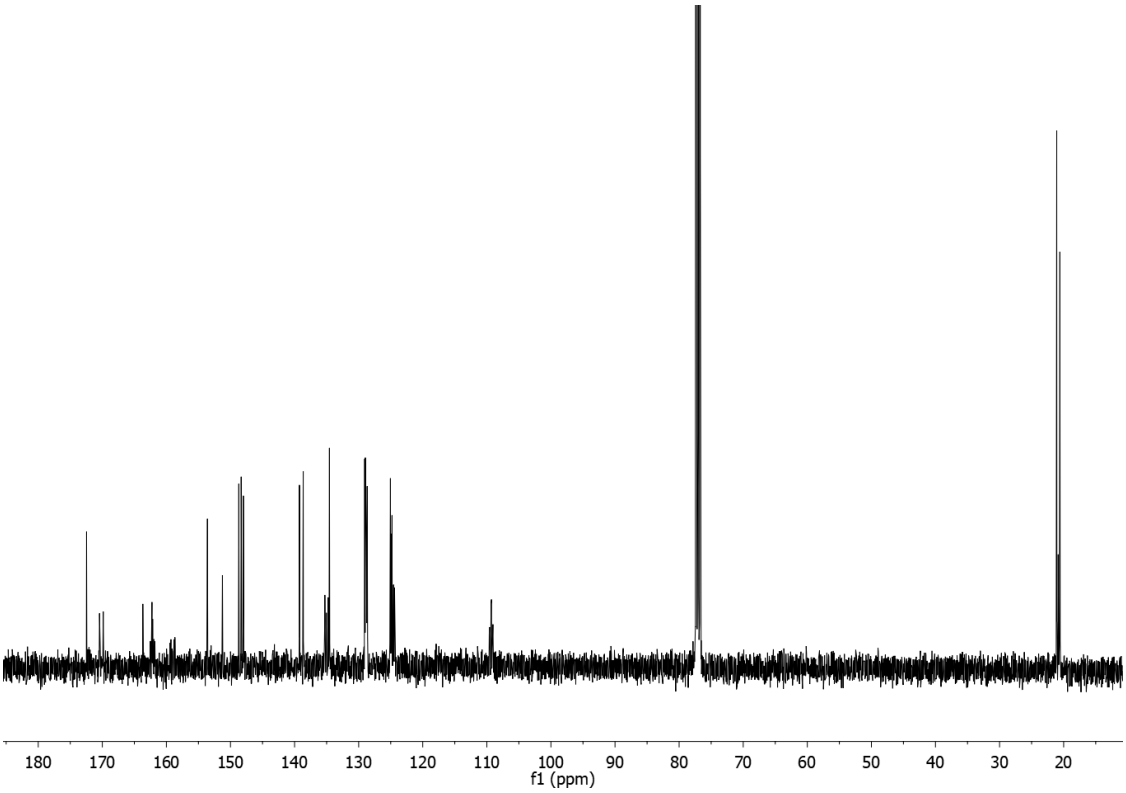

Figure S29: ^{13}C NMR spectrum of **2** in $CDCl_3$.

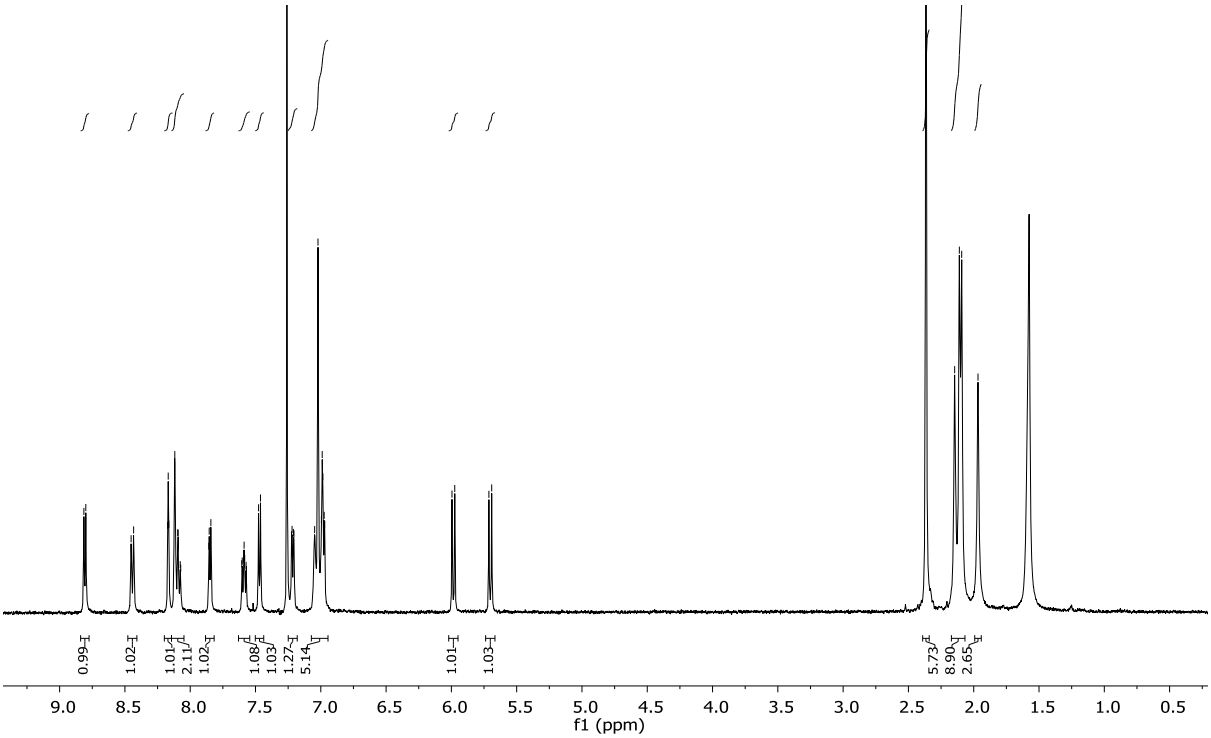

Figure S30: ^{1}H NMR spectrum of **3** in $CDCl_3$.

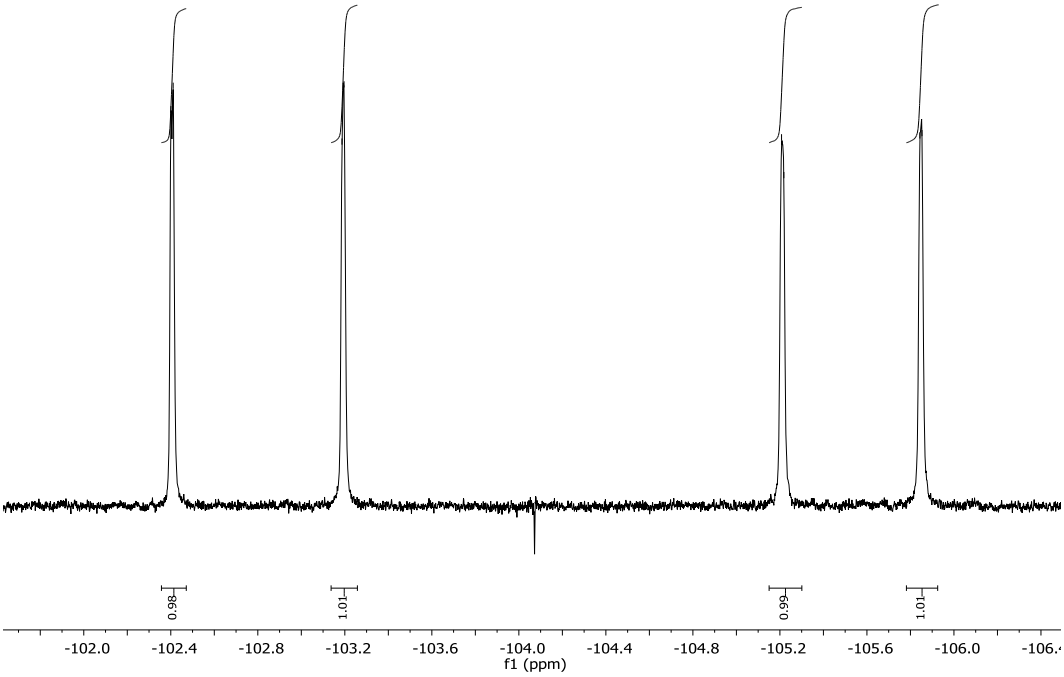

Figure S31: ^{19}F NMR spectrum of **3** in $CDCl_3$.

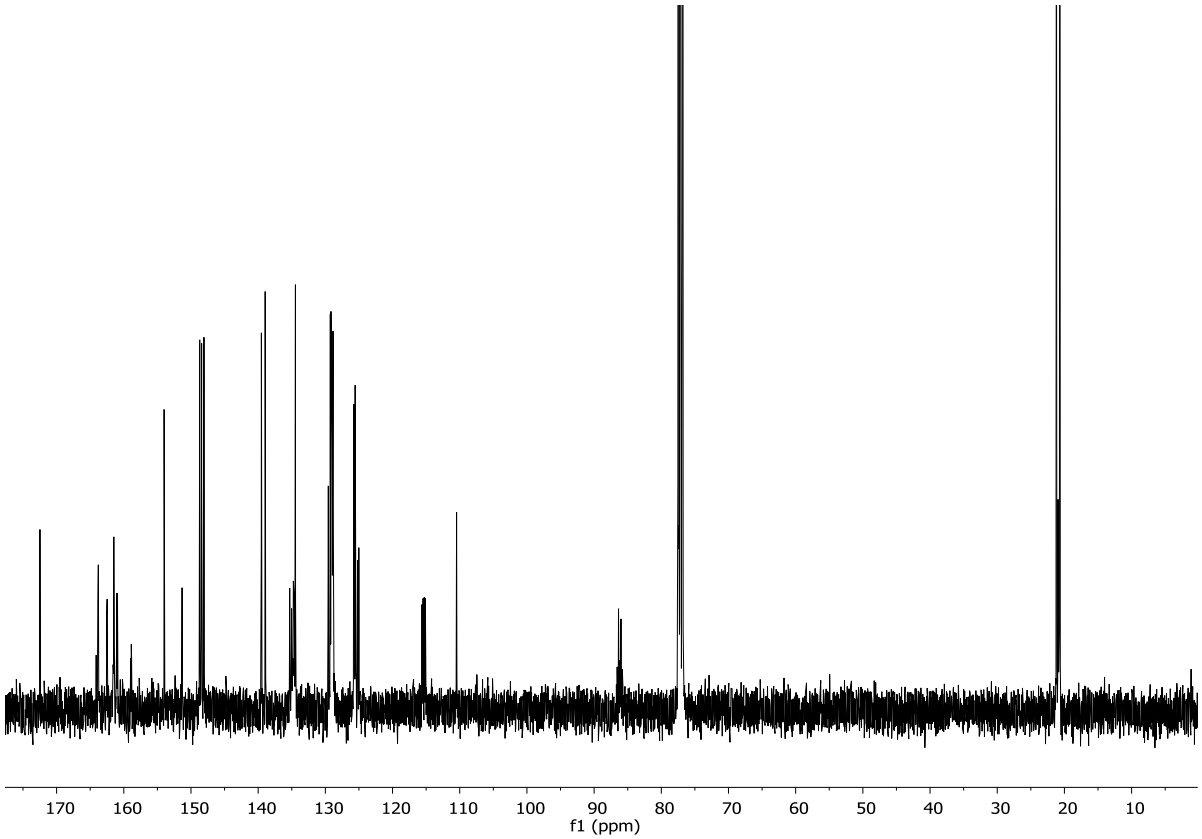

Figure S32: ^{13}C NMR spectrum of **3** in $CDCl_3$.

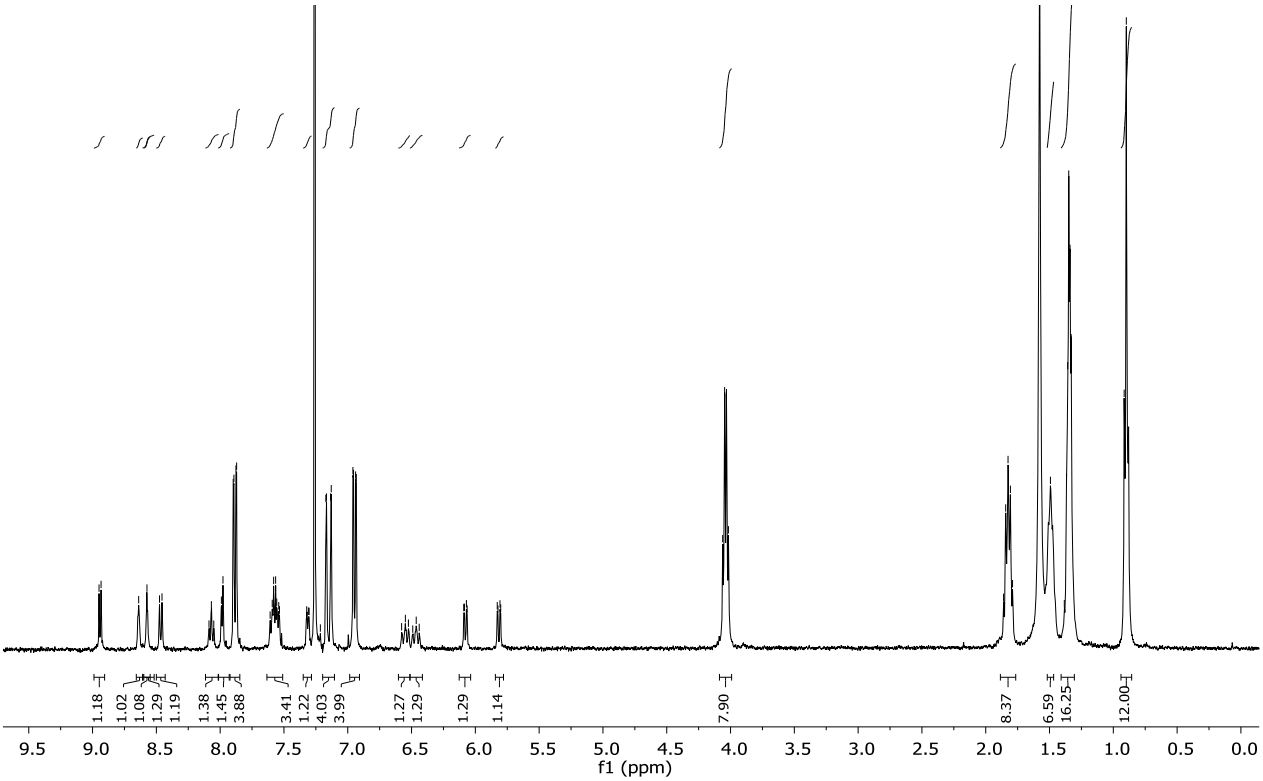

Figure S33: ^{1}H NMR spectrum of **4** in $CDCl_3$.

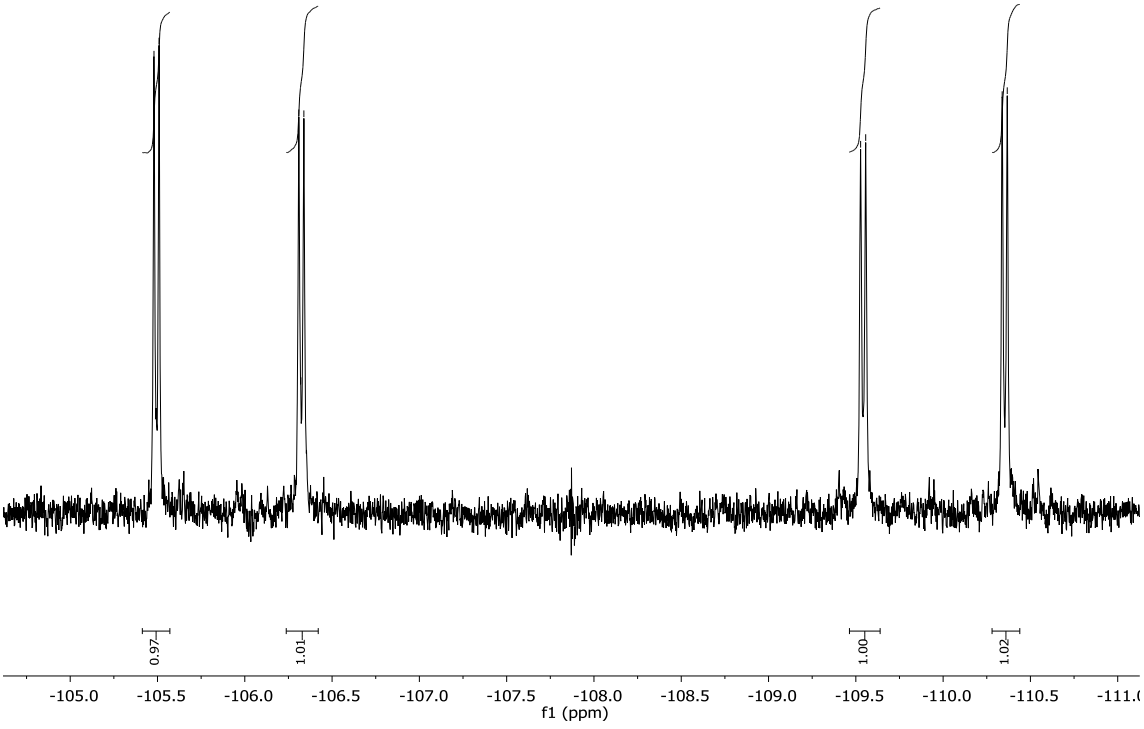

Figure S34 : ^{19}F NMR spectrum of **4** in $CDCl_3$.

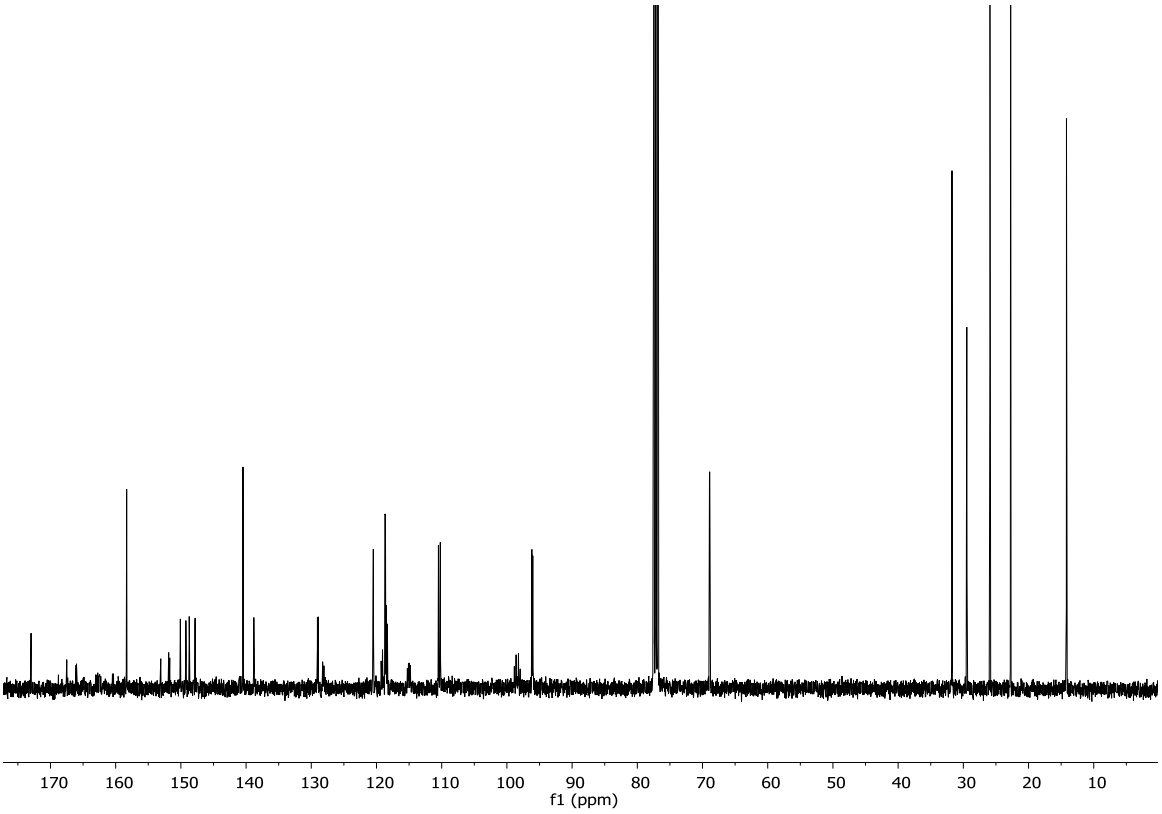

Figure S35: ^{13}C NMR spectrum of **4** in $CDCl_3$.

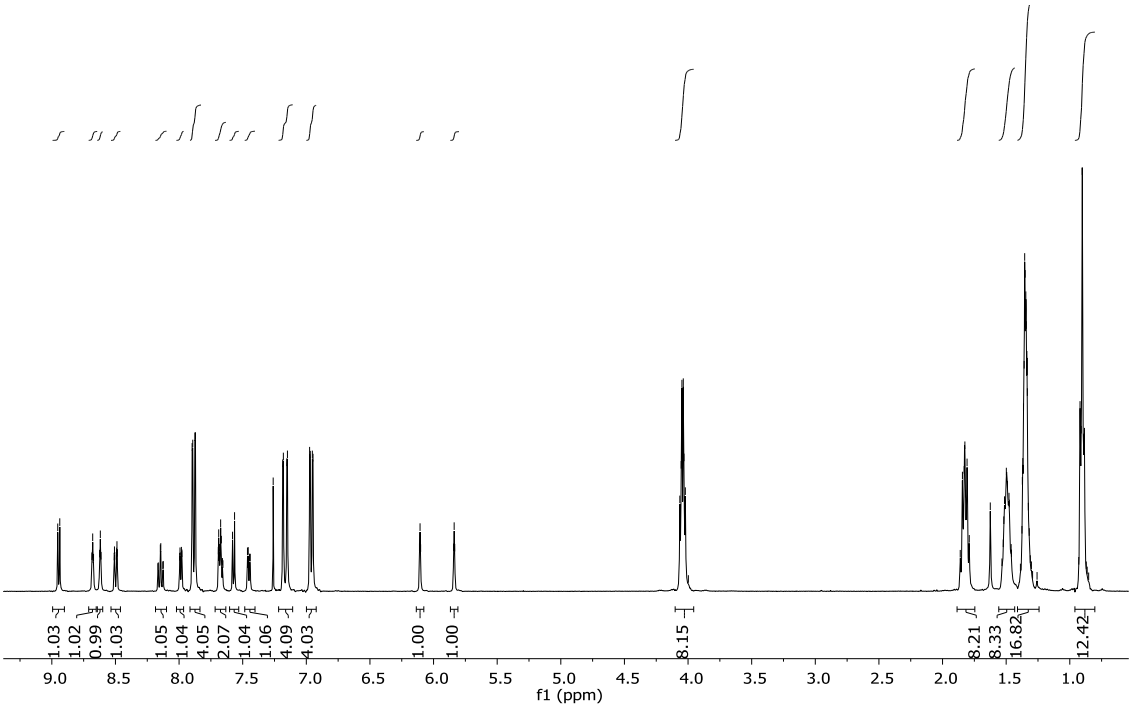

Figure S36: ^{1}H NMR spectrum of **5** in $CDCl_3$.

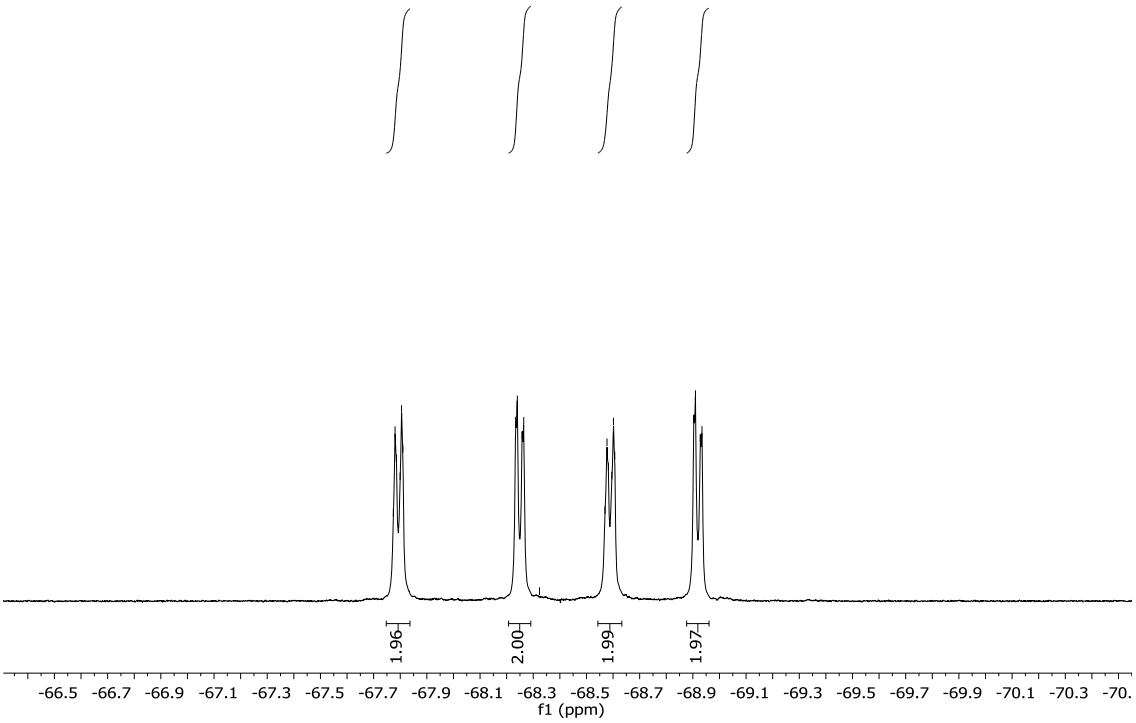

Figure S37: ^{19}F NMR spectrum of **5** in $CDCl_3$.

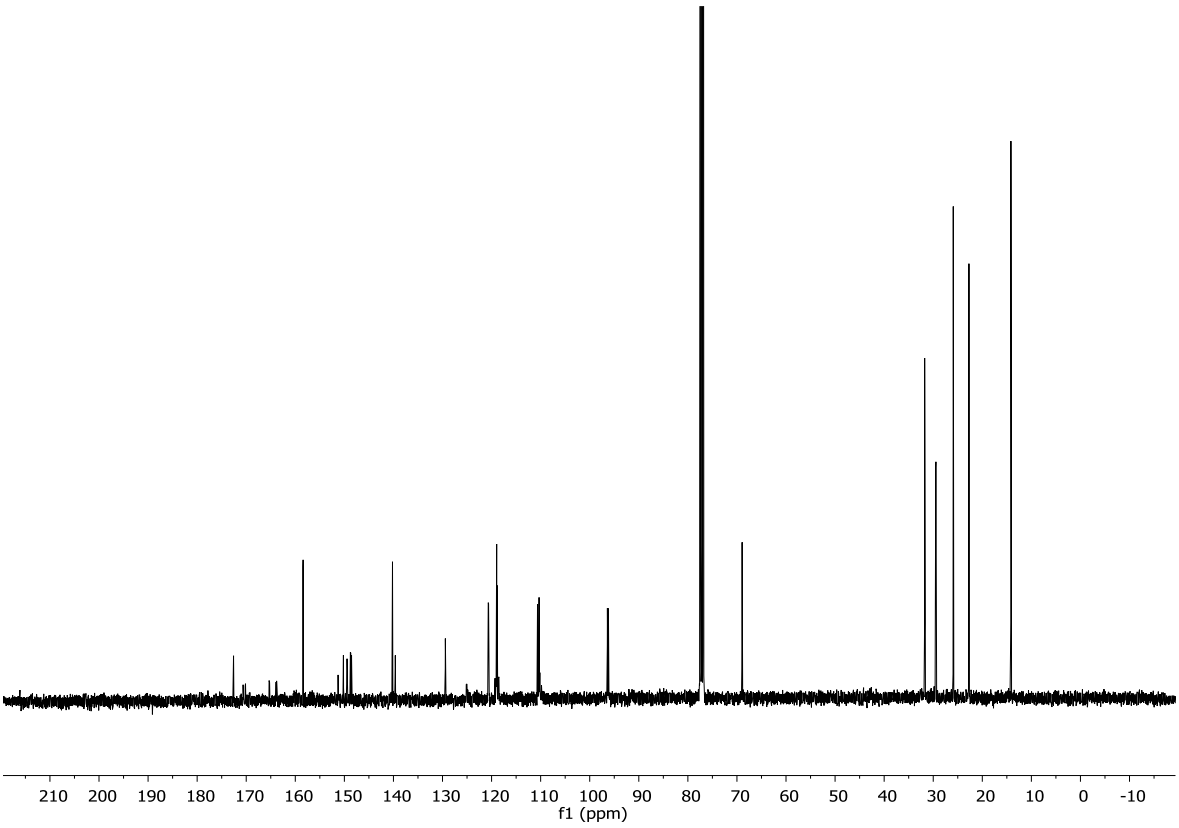

Figure S38: ^{13}C NMR spectrum of **5** in $CDCl_3$.

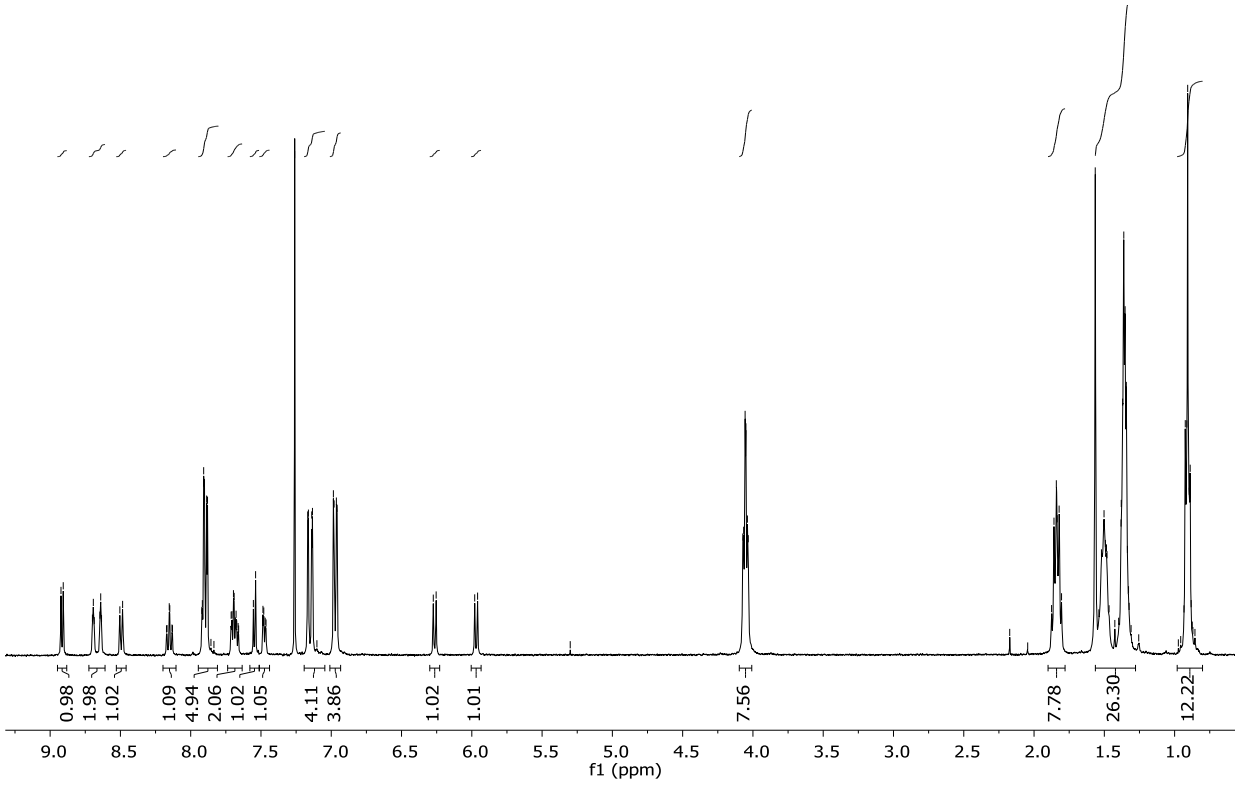

Figure S39: ^{1}H NMR spectrum of **6** in $CDCl_3$.

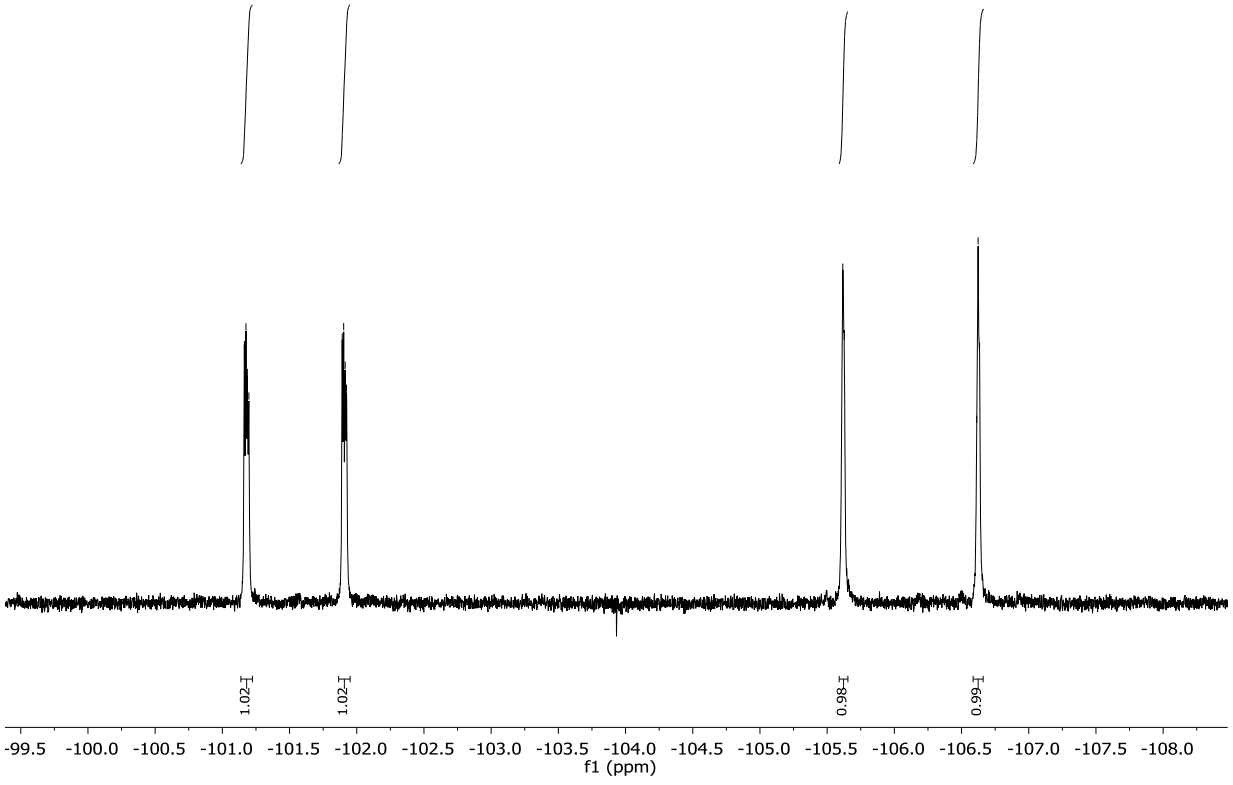

Figure S40: ^{19}F NMR spectrum of **6** in $CDCl_3$.

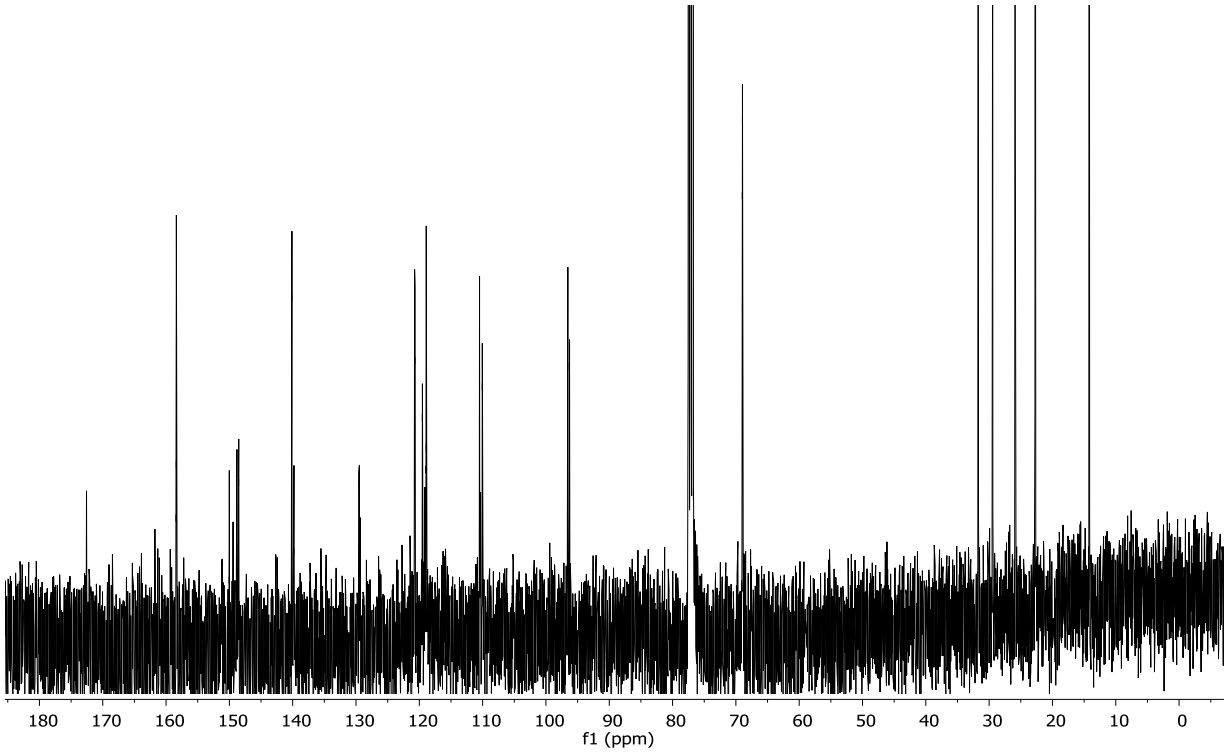

Figure S41: ^{13}C NMR spectrum of **6** in $CDCl_3$.

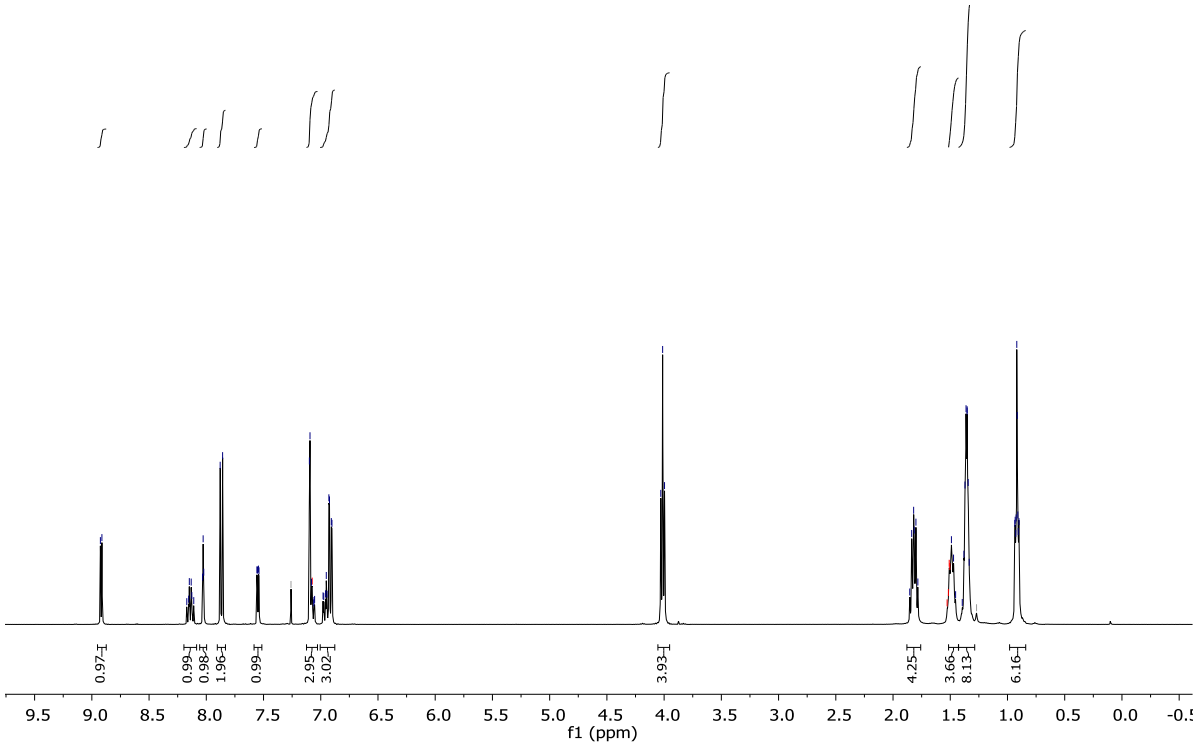

Figure S42: ^{1}H NMR spectrum of **9** in $CDCl_3$.

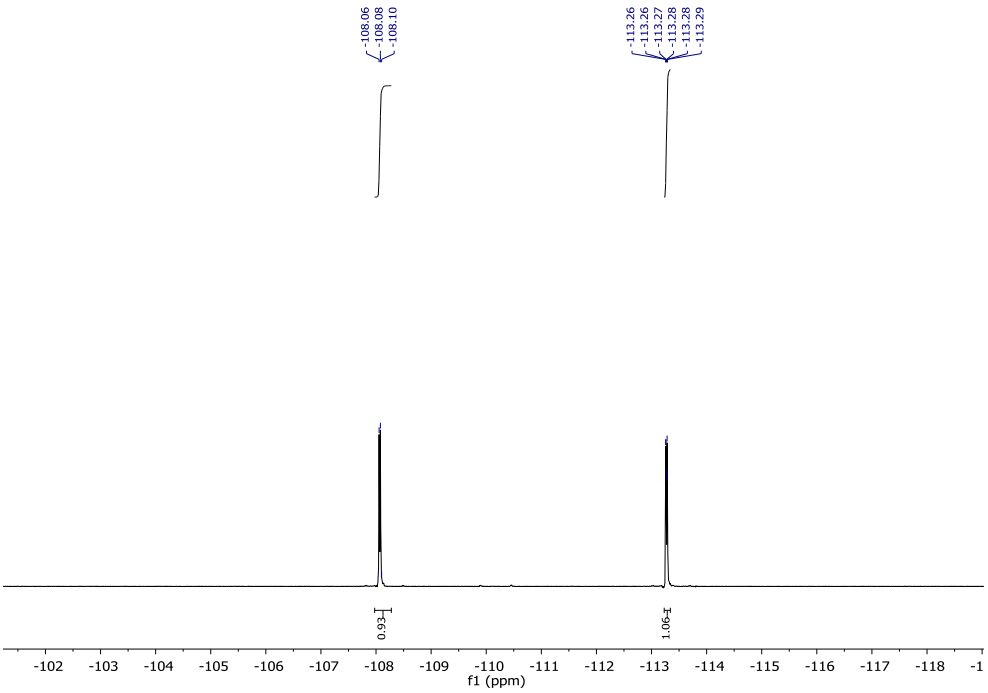

Figure S43: ^{19}F NMR spectrum of **9** in $CDCl_3$.

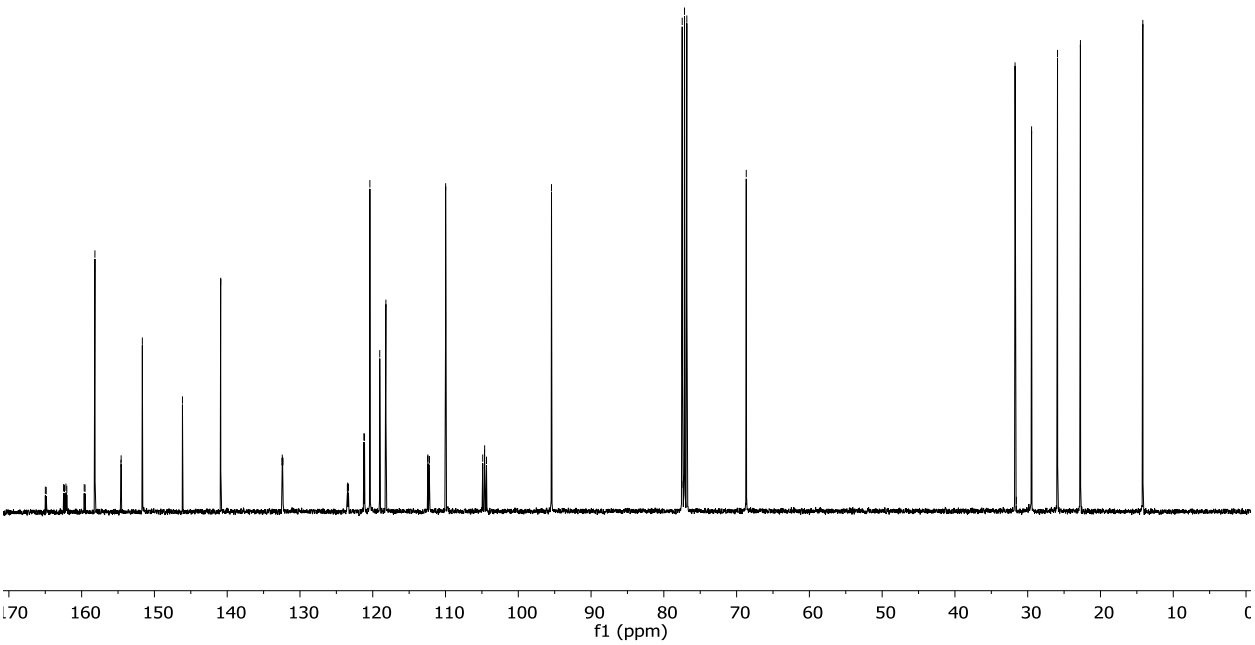

Figure S44: ^{13}C NMR spectrum of **9** in $CDCl_3$.

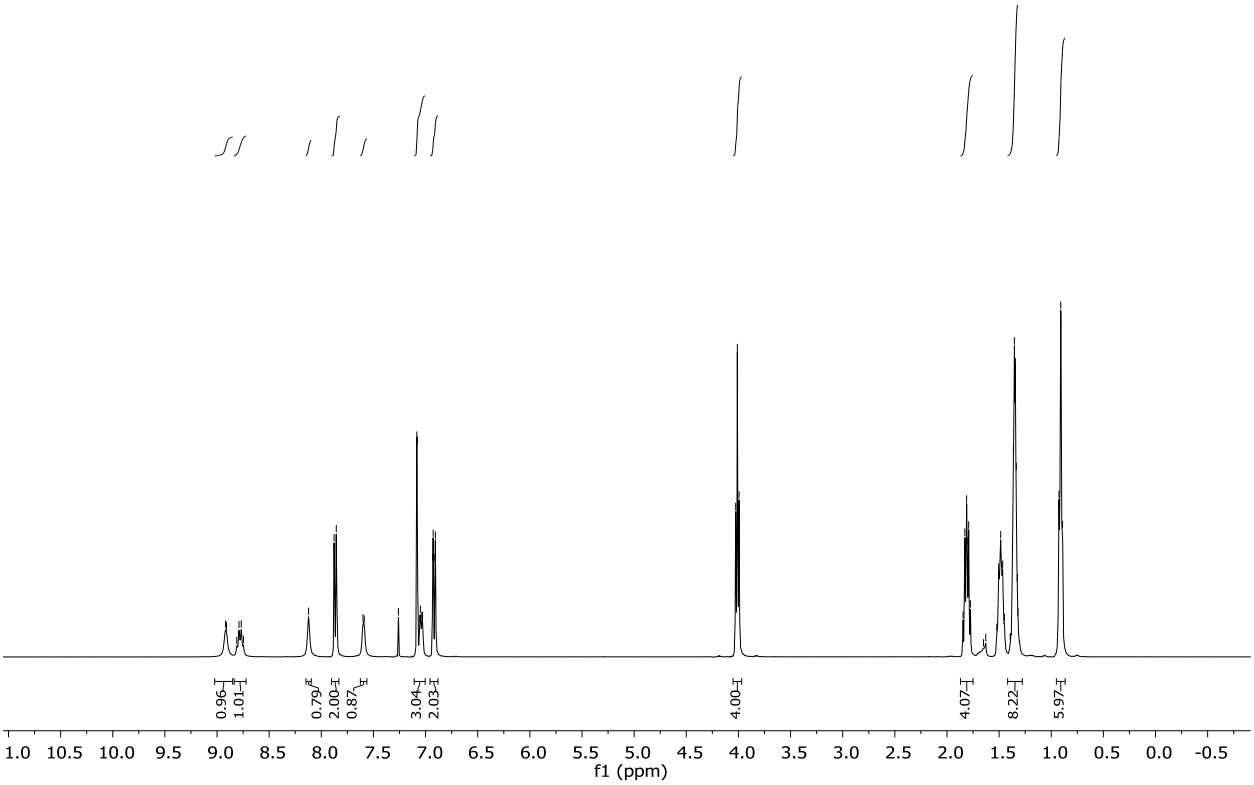

Figure S45: ^{1}H NMR spectrum of **10** in $CDCl_3$.

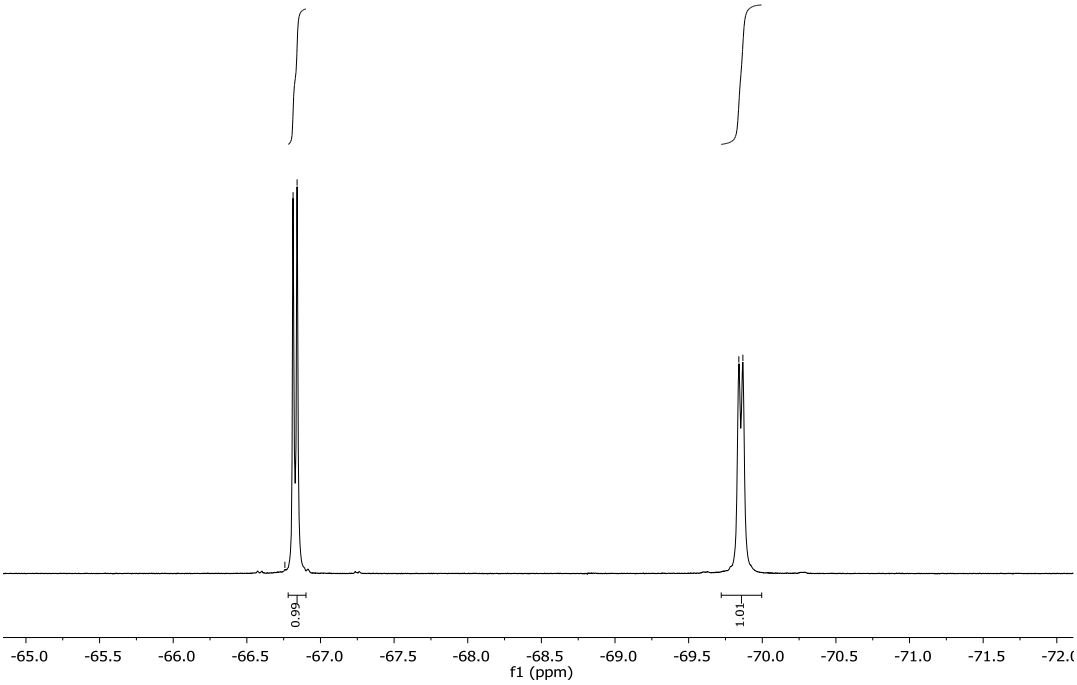

Figure S46: ^{19}F NMR spectrum of **10** in $CDCl_3$.

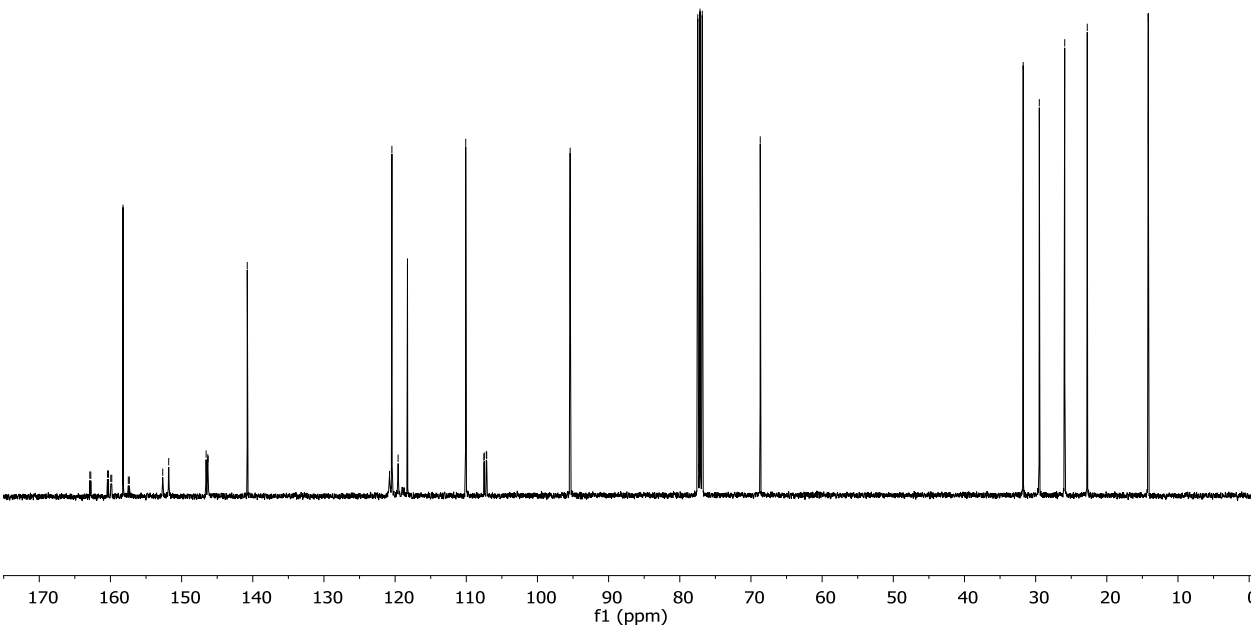

Figure S47: ^{13}C NMR spectrum of **10** in $CDCl_3$.

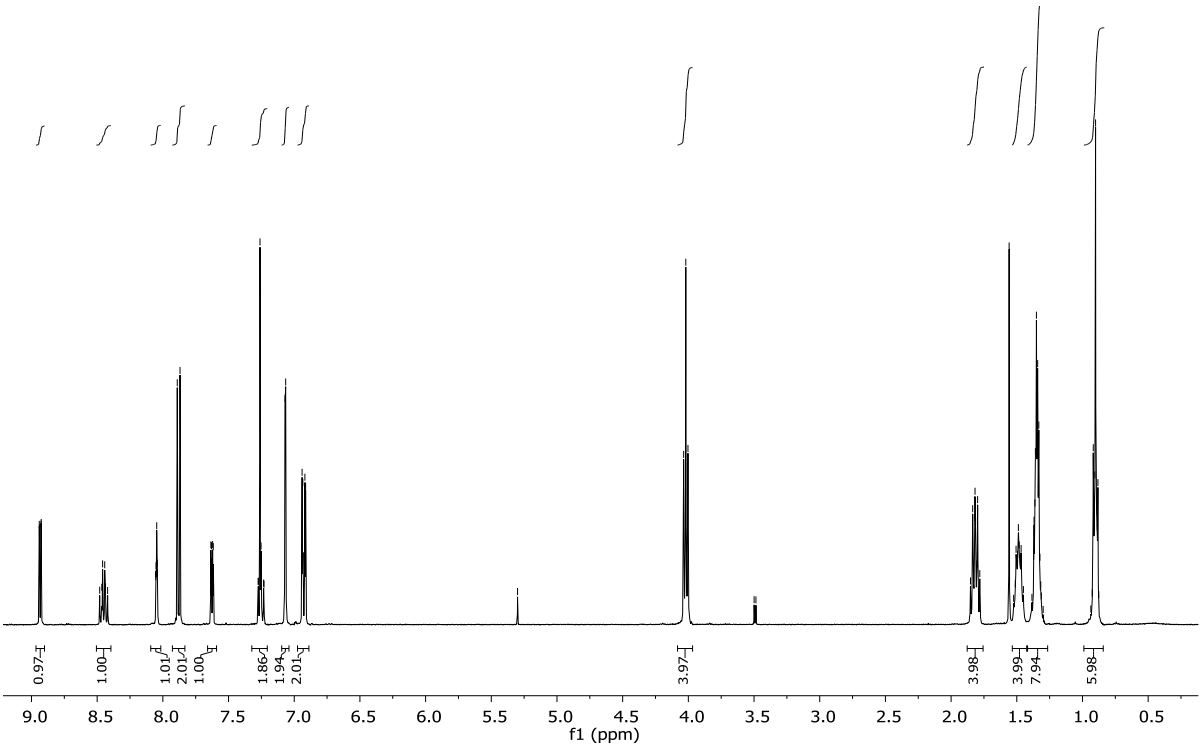

Figure S48: ^{1}H NMR spectrum of **11** in $CDCl_3$.

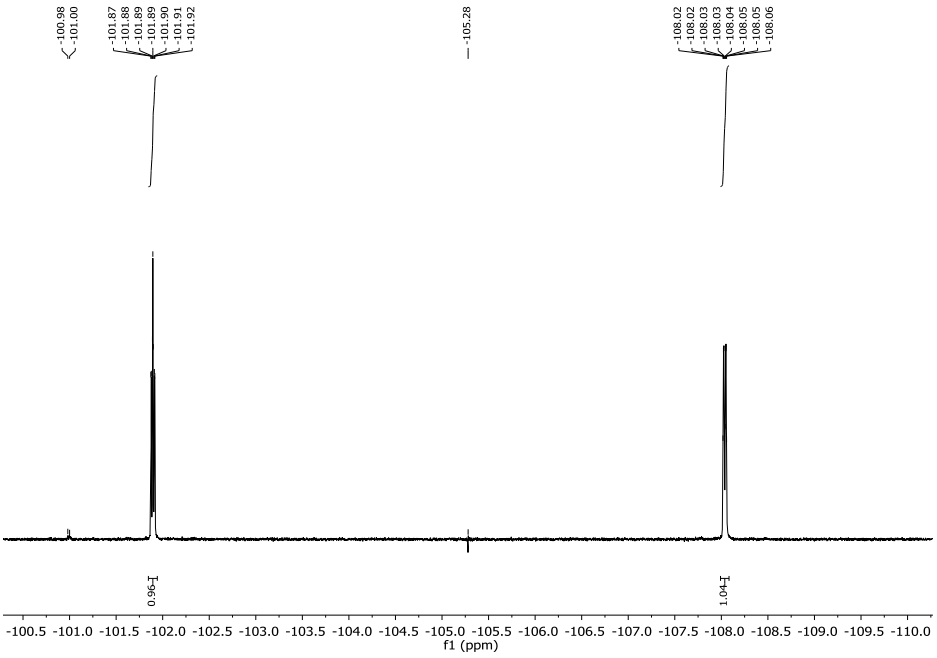

Figure S49: ^{19}F NMR spectrum of **11** in $CDCl_3$.

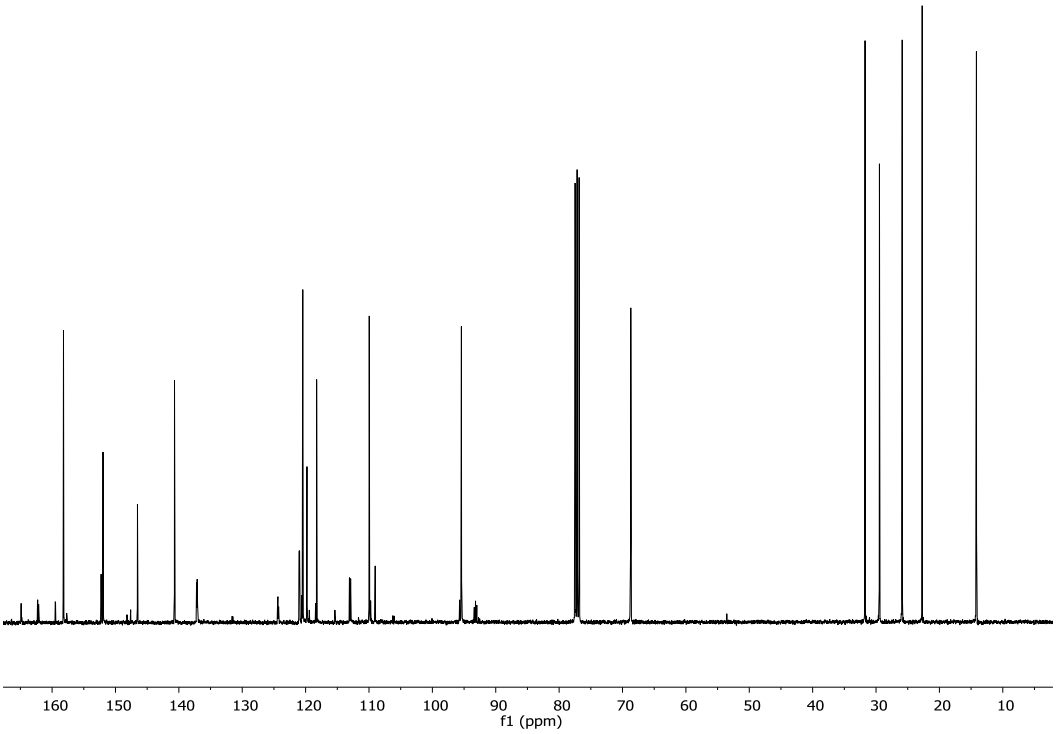

Figure S50: ^{13}C NMR spectrum of **11** in $CDCl_3$

References for the Supporting Information

1 V. N. Kozhevnikov, K. Dahms and M. R. Bryce, *J. Org. Chem.*, 2011, **76**, 5143–5148.

2 G. M. Sheldrick, *Acta Crystallogr. Sect. A Found. Crystallogr.*, 2008, 64, 112–122.

3 G. M. Sheldrick, *Acta Crystallogr. Sect. A Found. Adv.*, 2015, **71**, 3–8.

4 G. M. Sheldrick, *Acta Crystallogr. Sect. C Struct. Chem.*, 2015, **71**, 3–8.

5 O. V. Dolomanov, L. J. Bourhis, R. J. Gildea, J. A. K. Howard and H. Puschmann, *J. Appl. Crystallogr.*, 2009, **42**, 339–341.

6 B. Rees, L. Jenner and M. Yusupov, *Acta Crystallogr. Sect. D Biol. Crystallogr.*, 2005, **61**, 1299–1301.

7 M.-L. Xu, G.-B. Che, X.-Y. Li and Q. Xiao, *Acta Crystallogr. Sect. E Struct. Reports Online*, 2009, **65**, m28–m28.

8 T.-Y. Li, Y.-M. Jing, X. Liu, Y. Zhao, L. Shi, Z. Tang, Y.-X. Zheng and J.-L. Zuo, *Sci. Rep.*, 2015, **5**, 14912.

9 E. Baranoff, B. F. E. Curchod, F. Monti, F. Steimer, G. Accorsi, I. Tavernelli, U. Rothlisberger, R. Scopelliti, M. Grätzel and M. K. Nazeeruddin, *Inorg. Chem.*, 2012, **51**, 799–811.

10 Y. Zhao, J. Tang, H. Zhang and Y. Ma, *Eur. J. Inorg. Chem.*, 2014, **2014**, 4843–4851.

11 A. Maggiore, M. Pugliese, F. Di Maria, G. Accorsi, M. Gazzano, E. Fabiano, V. Tasco, M. Esposito, M. Cuscunà, L. Blasi, A. Capodilupo, G. Ciccarella, G. Gigli and V. Maiorano, *Inorg. Chem.*, 2016, **55**, 6532–6538.

12 R. D. Sanner and V. G. Young, *Acta Crystallogr. Sect. E Crystallogr. Commun.*, 2018, **74**, 1467–1470.